AGU PUBLICATIONS

JGR

Journal of Geophysical Research: Atmospheres

RESEARCH ARTICLE
10.1002/2015JD023908

Key Points:
- First experimental survey of new particle formation rates spanning free tropospheric conditions
- Addition of NH_3 in the low pptv-range strongly enhances new particle formation at low temperature
- Ion-induced nucleation is most efficient at temperatures of 248 K and higher

Supporting Information:
- Supporting Information S1

Correspondence to:
A. Kürten,
kuerten@iau.uni-frankfurt.de

Citation:
Kürten, A., et al. (2016), Experimental particle formation rates spanning tropospheric sulfuric acid and ammonia abundances, ion production rates, and temperatures, *J. Geophys. Res. Atmos.*, *121*, 12,377–12,400, doi:10.1002/2015JD023908.

Received 8 JUL 2015
Accepted 30 APR 2016
Published online 27 OCT 2016

Experimental particle formation rates spanning tropospheric sulfuric acid and ammonia abundances, ion production rates, and temperatures

Andreas Kürten[1], Federico Bianchi[2,3,4], Joao Almeida[1,5], Oona Kupiainen-Määttä[4], Eimear M. Dunne[6,7], Jonathan Duplissy[4,5], Christina Williamson[1,8], Peter Barmet[2], Martin Breitenlechner[9,10], Josef Dommen[2], Neil M. Donahue[11], Richard C. Flagan[12], Alessandro Franchin[4], Hamish Gordon[5], Jani Hakala[4], Armin Hansel[9,10], Martin Heinritzi[1], Luisa Ickes[1,3], Tuija Jokinen[4], Juha Kangasluoma[4], Jaeseok Kim[13], Jasper Kirkby[1,5], Agnieszka Kupc[8,14], Katrianne Lehtipalo[2,4], Markus Leiminger[1], Vladimir Makhmutov[15], Antti Onnela[5], Ismael K. Ortega[4,16], Tuukka Petäjä[4], Arnaud P. Praplan[2,17], Francesco Riccobono[2], Matti P. Rissanen[4], Linda Rondo[1], Ralf Schnitzhofer[9,10], Siegfried Schobesberger[4,18], James N. Smith[13,19], Gerhard Steiner[4,9,14], Yuri Stozhkov[15], António Tomé[20], Jasmin Tröstl[2], Georgios Tsagkogeorgas[21], Paul E. Wagner[14], Daniela Wimmer[1,4], Penglin Ye[11], Urs Baltensperger[2], Ken Carslaw[6], Markku Kulmala[4], and Joachim Curtius[1]

[1]Institute for Atmospheric and Environmental Sciences, Goethe University Frankfurt, Frankfurt am Main, Germany, [2]Laboratory of Atmospheric Chemistry, Paul Scherrer Institute, Villigen, Switzerland, [3]Institute of Atmospheric and Climate Science, ETH Zurich, Zurich, Switzerland, [4]Department of Physics, University of Helsinki, Helsinki, Finland, [5]Physics Department, CERN, Geneva, Switzerland, [6]School of Earth and Environment, University of Leeds, Leeds, UK, [7]Atmospheric Research Centre of Eastern Finland, Finnish Meteorological Institute, Kuopio, Finland, [8]Cooperative Institute for Research in Environmental Sciences, University of Colorado Boulder, Boulder, Colorado, USA, [9]Institute for Ion and Applied Physics, University of Innsbruck, Innsbruck, Austria, [10]Ionicon Analytik GmbH, Innsbruck, Austria, [11]Center for Atmospheric Particle Studies, Carnegie Mellon University, Pittsburgh, Pennsylvania, USA, [12]Division of Chemistry and Chemical Engineering, California Institute of Technology, Pasadena, California, USA, [13]Department of Applied Physics, University of Eastern Finland, Kuopio, Finland, [14]Faculty of Physics, University of Vienna, Vienna, Austria, [15]Solar and Cosmic Ray Research Laboratory, Lebedev Physical Institute, Moscow, Russia, [16]Onera-The French Aerospace Lab, Palaiseau, France, [17]Finnish Meteorological Institute, Helsinki, Finland, [18]Department of Atmospheric Sciences, University of Washington, Seattle, Washington, USA, [19]Department of Chemistry, University of California, Irvine, California, USA, [20]SIM, University of Lisbon and University of Beira Interior, Lisbon, Portugal, [21]Leibniz Institute for Tropospheric Research, Leipzig, Germany

Abstract Binary nucleation of sulfuric acid and water as well as ternary nucleation involving ammonia are thought to be the dominant processes responsible for new particle formation (NPF) in the cold temperatures of the middle and upper troposphere. Ions are also thought to be important for particle nucleation in these regions. However, global models presently lack experimentally measured NPF rates under controlled laboratory conditions and so at present must rely on theoretical or empirical parameterizations. Here with data obtained in the European Organization for Nuclear Research CLOUD (Cosmics Leaving OUtdoor Droplets) chamber, we present the first experimental survey of NPF rates spanning free tropospheric conditions. The conditions during nucleation cover a temperature range from 208 to 298 K, sulfuric acid concentrations between 5×10^5 and 1×10^9 cm^{-3}, and ammonia mixing ratios from zero added ammonia, i.e., nominally pure binary, to a maximum of ~1400 parts per trillion by volume (pptv). We performed nucleation studies under pure neutral conditions with zero ions being present in the chamber and at ionization rates of up to 75 ion pairs cm^{-3} s^{-1} to study neutral and ion-induced nucleation. We found that the contribution from ion-induced nucleation is small at temperatures between 208 and 248 K when ammonia is present at several pptv or higher. However, the presence of charges significantly enhances the nucleation rates, especially at 248 K with zero added ammonia, and for higher temperatures independent of NH_3 levels. We compare these experimental data with calculated cluster formation rates from the Atmospheric Cluster Dynamics Code with cluster evaporation rates obtained from quantum chemistry.

1. Introduction

Formation of new particles is an important process in Earth's atmosphere, affecting cloud formation, visibility, climate, air chemistry, and human health [*Lohmann and Feichter*, 2005; *Andreae and Crutzen*, 1997; *Nel*, 2005]. New particle formation events have been observed at many different locations [*Kulmala et al.*, 2004], e.g., in

polluted areas [*Brock et al.*, 2002; *Stanier et al.*, 2004; *Chen et al.*, 2012], in forests [*Kulmala et al.*, 2013], in Arctic regions [*Laakso et al.*, 2003], marine areas [*Weber et al.*, 1998; *O'Dowd et al.*, 1998], and in the free troposphere [*Brock et al.*, 1995; *de Reus et al.*, 2000; *Lee et al.*, 2003; *Weigel et al.*, 2011; *Bianchi et al.*, 2016]. It is not completely understood which vapors are responsible for nucleation and growth, although a correlation with the concentration of gas-phase sulfuric acid generally exists [*Weber et al.*, 1999; *Sihto et al.*, 2006; *Kuang et al.*, 2008]. However, the binary system of sulfuric acid and water vapor cannot account for atmospheric boundary layer nucleation events at typical midlatitude temperatures [*Weber et al.*, 1996; *Kirkby et al.*, 2011; *Duplissy et al.*, 2016]. Therefore, in these regions ternary vapors are required in order to explain the observed nucleation rates.

One commonly proposed stabilizing agent is ammonia [*Coffman and Hegg*, 1995; *Larsen et al.*, 1997; *Korhonen et al.*, 1999]. Several experimental studies have shown that the presence of NH_3 can lead to an enhancement in nucleation rates [*Ball et al.*, 1999; *Hanson and Eisele*, 2002; *Benson et al.*, 2009; *Kirkby et al.*, 2011; *Zollner et al.*, 2012; *Froyd and Lovejoy*, 2012], in agreement with theoretical predications based on quantum chemistry, which show that sulfuric acid clusters are stabilized due to the presence of ammonia [*Torpo et al.*, 2007; *Ortega et al.*, 2012]. However, despite the ability of ammonia to act as a stabilizing compound, nucleation rates observed for the ternary system that included NH_3 are still too low to explain most boundary layer nucleation events [*Kirkby et al.*, 2011].

Another potential stabilizing agent is charge. The effect of ions on nucleation has long been debated; conflicting data exist as to whether or not ion-induced nucleation (IIN) is important on a global scale [*Yu and Turco*, 2000; *Kazil et al.*, 2008; *Manninen et al.*, 2009]. *Kirkby et al.* [2011] showed that for both the nominally binary H_2SO_4-H_2O system (i.e., where the concentration of gas-phase ammonia was below the detection limit but where ammonia could not be strictly ruled out from particle formation) between 248 and 292 K, and the ternary H_2SO_4-H_2O-NH_3 system between 278 and 292 K, the presence of ions leads to significantly enhanced nucleation rates. *Duplissy et al.* [2016] investigated the binary system between 208 and 298 K, using high-resolution mass spectrometry to distinguish between the nominally binary system and the pure binary system. The authors found that the binary formation rates increase with relative humidity (RH), sulfuric acid, and ion concentration and decrease with temperature. Under atmospheric conditions neutral particle formation dominates at low temperatures, while ion-induced particle formation dominates at higher temperatures.

Other stabilizing agents considered more recently are amines (mainly dimethylamine, $(CH_3)_2NH$), which, in theory, are much more efficient than ammonia in lowering the evaporation rates of sulfuric acid clusters [*Kurtén et al.*, 2008; *Ortega et al.*, 2012]. The high efficiency of amines to stabilize acidic clusters has also been demonstrated experimentally in recent studies [*Bzdek et al.*, 2010; *Erupe et al.*, 2011; *Chen et al.*, 2012; *Zollner et al.*, 2012; *Almeida et al.*, 2013; *Jen et al.*, 2014; *Kürten et al.*, 2014]. The study by *Almeida et al.* [2013] showed that typical atmospheric boundary layer new particle formation rates are compatible with nucleation rates in the ternary system involving dimethylamine at representative atmospheric levels: amine mixing ratios of a few parts per trillion by volume (pptv) for a temperature of 278 K, and sulfuric acid concentrations between ~2×10^6 and 1×10^7 cm^{-3}. However, this result does not rule out an influence from other compounds, such as oxidized organics, that can explain typical ground-level nucleation rates [*Zhang et al.*, 2004; *Metzger et al.*, 2010; *Riccobono et al.*, 2012; *Schobesberger et al.*, 2013; *Riccobono et al.*, 2014; *Kirkby et al.*, 2016]. The exact mechanisms leading to the highly oxidized compounds in these systems need to be resolved, as does the question at what cluster size these compounds become important for nucleation and growth.

Many of the above-mentioned studies have focused on explaining nucleation rates at the surface, where ternary organic vapors or strong bases seem to be necessary to reproduce the measured nucleation rates. However, the free troposphere is likely to be more important for the Earth's climate. In the free troposphere, nucleation has frequently been observed [*Weber et al.*, 1999; *Clarke et al.*, 1999; *Boulon et al.*, 2010; *Rose et al.*, 2015a, 2015b; *Bianchi et al.*, 2016]; in models, it accounts for 35% of cloud condensation nuclei in low-level clouds [*Merikanto et al.*, 2009]. Although binary and ternary ammonia nucleation rates are not high enough under the warm conditions of the boundary layer, they are much higher at the lower temperatures of the middle and upper troposphere. Ternary organic vapors are likely present at lower concentrations in these regions, i.e., with increasing distance from their sources in the boundary layer, and could therefore be less important. Furthermore, ionization rates in the upper troposphere can be higher, leading to significant ion-induced nucleation. Indications that ion-induced nucleation is important in these regions have been reported [*Lee et al.*, 2003; *Weigel et al.*, 2011].

Table 1. Parameter Space Explored During CLOUD3 (October/November 2010), CLOUD5 (October/November 2011), and CLOUD7 (October–December 2012)

Parameter	Range
Temperature	208 to 298 K
$[H_2SO_4]$	$\sim 5 \times 10^5$ to 1×10^9 cm^{-3}
$[NH_3]$	[a] $\sim 10^{-2}$ to $\sim 1.4 \times 10^3$ pptv
Ion concentration	0 (neutral) to $\sim 5 \times 10^3$ cm^{-3}

[a]The lowest ammonia concentrations under nominally binary conditions were not directly measured (see text for details).

This study focuses extensively on the binary and ternary ammonia system by extending the parameter space to temperatures as low as 208 K. This temperature range covers high-latitude regions as well as middle and upper tropospheric conditions. Like sulfur dioxide, ammonia concentrations are strongly associated with anthropogenic activity. The emissions from livestock waste, NH_3-based-fertilizers, biomass burning, and crops account for much of the total ammonia emissions. Human activity has led to a substantial increase in total ammonia emissions since preindustrial times, and a significant further increase is expected to occur in the future [*Krupa*, 2003; *Clarisse et al.*, 2009]. Ammonia is therefore an important compound to study due to its potential climate impacts. It is also of interest to assess the impact of ions on new particle formation for a wide range of conditions.

Here the experimentally determined formation rates of pure binary nucleation from *Duplissy et al.* [2016] are extended to the ternary ammonia system. We present experimentally determined nucleation rates that were obtained during three different campaigns conducted at the European Organization for Nuclear Research (CERN) CLOUD (Cosmics Leaving OUtdoor Droplets) chamber. The measurements were made during CLOUD3 (October/November 2010), CLOUD5 (October/November 2011), and CLOUD7 (October–December 2012). For the data analysis, ammonia calibration measurements from CLOUD6 (June 2012) were used. The investigated parameter space covers a wide range of tropospheric conditions and is summarized in Table 1. The relative humidity (RH) was sometimes varied (at 223 K, see Text S3 in the supporting information and at 298 K, see section 3.1.6) but no systematic investigation of the RH effect was performed; for most experiments the RH was set to 38%. We present nucleation rates as a function of the sulfuric acid concentration, ammonia mixing ratio, and temperature, as well as charge enhancement factors for ion-induced nucleation under the influence of galactic cosmic rays (GCR), and amplified by the CERN pion beam. Part of the data (from CLOUD3) were previously presented by *Kirkby et al.* [2011]. However, these older data present only a small subset of the formation rates shown in this study and were limited to temperatures of 248 K, 278 K, and 292 K for the nominally binary system and to 278 and 292 K for the ternary system.

Using cluster collision and evaporation rates, the formation rates of nucleating clusters can be calculated. However, especially the direct measurement of evaporation rates for individual clusters as a function of temperature is challenging and the data availability is limited. Therefore, quantum chemical studies are essential in obtaining those rate constants [e.g., *Ortega et al.*, 2012]. The measurements from this study are compared to calculated particle formation rates from the Atmospheric Cluster Dynamics Code (ACDC) using cluster evaporation rates obtained from quantum chemistry [*McGrath et al.*, 2012].

2. Methods

2.1. CLOUD Chamber and Instruments

The effect of ionizing radiation on new particle formation and aerosol growth is investigated by CLOUD [*Kirkby et al.*, 2011]. A key feature of CLOUD is that its experimental conditions are extremely well controlled, and the experiments are performed in a way that attempts to minimize the concentration of potential contaminants [*Schnitzhofer et al.*, 2014]. The CLOUD chamber consists of a stainless steel cylinder with a volume of 26.1 m^3 that is electropolished on the inside; it is described in detail by *Duplissy et al.* [2016]. A thermal housing is used to circulate air in between the chamber and its insulation. The internal chamber temperature can be controlled precisely to within several hundredths of a degree by this arrangement. UV light that is used to initiate photochemical reactions is brought into the chamber by means of a sophisticated fiber-optic light system. The UV light system has been carefully characterized; no measureable increase in temperature is observed when the light is turned on [*Kupc et al.*, 2011]. Air from cryogenic supplies, i.e., N_2 and O_2 that should contain a minimum of condensable contaminants, is mixed at a ratio of 79:21 before it is used to fill the chamber and replenish the gas taken by the instruments. The relative humidity can be adjusted by controlling the flow rate ratio of dry air, and the flow rate of air that has passed through a humidification system containing

ultrapure water. Trace gases like ozone and sulfur dioxide can also be added; their concentrations are adjusted with mass flow controllers. The air inside the chamber is continuously stirred by two mixing fans [*Voigtländer et al.*, 2012]. One fan is installed at the bottom and another one at the top while the fan speed is controlled by magnetically coupled motors located outside of the chamber. Two high-voltage grids can be used to sweep out all ions over a period of less than a second by applying an electrical field of 20 kV/m across the chamber. This enables purely neutral nucleation runs. If the high voltage field cage is grounded, natural radiation from galactic cosmic rays (GCR) provides an ionization rate of ~3 ion pairs cm^{-3} s^{-1}. Charged pions from the CERN proton synchrotron can be used to achieve mean ionization rates of up to ~75 cm^{-3} s^{-1} [*Franchin et al.*, 2015]. The beam is defocused such that an area of about 1.5×1.5 m^2 of the chamber is homogenously illuminated by the pions. Nucleation rates (J) can therefore be obtained either under neutral (J_n), galactic cosmic ray (J_{GCR}), or charged pion beam (J_π) conditions. In the case of the experiments under the influence of ions J_{GCR} and J_π represent the sum of the neutral nucleation rate and the ion-induced nucleation rate.

Nucleation experiments are initiated through the photolytic production of sulfuric acid. The photolysis of ozone leads to the generation of O^1D; subsequent reactions involving H_2O, SO_2, and O_2 generate sulfuric acid. The concentration of H_2SO_4 has been measured with a calibrated Chemical Ionization Mass Spectrometer at concentrations between $\sim 5 \times 10^5$ and $\sim 1 \times 10^9$ cm^{-3} [*Kürten et al.*, 2011, 2012]. The measurement of sulfuric acid monomers and neutral dimers at low temperatures during CLOUD5 is described elsewhere [*Kürten et al.*, 2015]. For experiments where ammonia was intentionally added to the chamber, a gas bottle of NH_3 diluted in nitrogen (1% of NH_3 in N_2, Carbagas) was used. The flow rate from this bottle and further flows of dry air for dilution were adjusted to achieve the desired mixing ratios (see Text S1). The instrumentation used to measure the ammonia comprised a LOng Path Absorption Photometer during CLOUD3 [*Bianchi et al.*, 2012], an ion chromatograph [*Praplan et al.*, 2012] during CLOUD5, CLOUD6, and CLOUD7, and a Proton Transfer Reaction-Mass Spectrometer using O_2^+ reagent ions [*Norman et al.*, 2007] during CLOUD3, CLOUD5, CLOUD6, and CLOUD7. The determination of NH_3 at concentrations below ~2 pptv and at temperatures lower than the freezing point of water is challenging due to instrumental limitations. This will be discussed in greater detail in Text S1. For the measurement of relative humidity a two-stage dew/frost-point mirror was used (EdgeTech). At very low temperatures where the frost point temperature reaches values around 203 K, it was necessary to utilize a three-stage frost point mirror (EdgeTech) for accurate measurements. An Atmospheric Pressure interface-Time Of Flight (APi-TOF) mass spectrometer determined the composition of ions with a mass-to-charge ratio up to about 3000 Th at a mass resolving power of ~5000 [*Junninen et al.*, 2010; *Schobesberger et al.*, 2015]. During CLOUD it provided information about the chemical identity of cluster ions during a nucleation experiment. It can be used to identify the extent to which ammonia was contained in the clusters in order to distinguish qualitatively between pure binary nucleation and nucleation that is influenced by the presence of contaminant ammonia [*Duplissy et al.*, 2016; *Schobesberger et al.*, 2015]. The concentrations of ozone and sulfur dioxide were measured with commercial gas monitors (TEI 49C, Thermo Environmental Instruments and Enhanced Trace Level SO_2 Analyzer, Model 43i-TLE, Thermo Scientific). The pressure inside the CLOUD chamber was maintained at approximately 1.005 bar during all of the experiments.

The instruments used to determine the number density of aerosol particles included commercial condensation particle counters (CPCs, TSI, Inc.) with different cutoff sizes starting at 3.2 nm, two di-ethylene glycol-based CPCs [*Iida et al.*, 2009; *Wimmer et al.*, 2013] with cutoff sizes between 2 and 2.7 nm and two particle size magnifiers [*Vanhanen et al.*, 2011] with cutoff sizes between ~1.3 and 1.8 nm. The particle size distribution was measured in the range between 4 and 100 nm with a scanning mobility particle sizer (SMPS) and with a neutral cluster and air ion spectrometer (NAIS) [*Mirme and Mirme*, 2013]. The NAIS provided additional information about the negative and positive small ion and particle concentrations in a size range between 0.8 and 42 nm [*Franchin et al.*, 2015].

2.2. Determination of the Nucleation Rate $J_{1.7}$

In accordance with previous CLOUD publications a mobility diameter of 1.7 nm has been chosen as the reference size for the reported particle formation rates [*Kirkby et al.*, 2011; *Almeida et al.*, 2013]. This mobility diameter corresponds to about 1200 atomic mass units (for a density of 1500 kg m^{-3} [*Ehn et al.*, 2011]) and should be above the critical size for all conditions examined. The critical size corresponds to the cluster/particle that is at least as likely to grow as to evaporate. Since this definition is ambiguous in a multicomponent system, in this study, we refer to the sulfuric acid coordinate, i.e., the loss and gain of sulfuric acid molecules, when speaking about the critical size.

We derive $J_{1.7}$ from particle number density measurements in a two-step process. First, we determine $J_{3.2}$ (the particle formation rate at 3.2 nm, see Text S2). This is based on a number balance between $N_{3.2}$, i.e., the total particle number $\geq$ 3.2 nm measured with an ultrafine CPC 3776 (TSI, Inc.) that has a 50% detection cutoff at 3.2 nm (d_{50}) and the particle losses above that cutoff size. In a second step the formation rate at 3.2 nm is used to calculate the formation rate at 1.7 nm ($J_{1.7}$) by accounting for particle losses occurring while particles grow from 1.7 to 3.2 nm (see Text S2 for the applied methods). This requires knowledge of the growth rate, as well as the loss processes in this size range. When data from instruments with detection thresholds between 1.3 and 2.7 nm are available, these are used to constrain the formation rates in this size range, but we can always calculate $J_{1.7}$ based solely on adjusting $J_{3.2}$ obtained from the CPC 3776. In general, the various methods agree to within a factor of 2, as shown in Figure S3 in the supporting information. For consistency, we use the $J_{1.7}$ values obtained from the CPC 3776 in this work.

During CLOUD3 when the chamber was operated at temperatures below 292 K, the particle counters were cooled to about 280 K to minimize the residence time of particles inside the warm instrument inlets and tubes. During CLOUD5, when the chamber temperature was as low as 208 K, the particle counters were contained in thermal huts, which were cooled to 243 K when the chamber was held at 208 or 223 K [*Wimmer et al.*, 2015]. Despite these efforts, we are aware that the measurements presented here for the low temperatures are potentially subject to uncorrected evaporation effects due to relatively warm instruments. However, to our knowledge no condensation particle counters presently exist that can be routinely operated isothermally at temperatures below 273 K.

When the aerosol passes through the capillary of the CPC conditions are such that the air has sufficient time to equilibrate to the warm conditions of the CPC before it enter the condenser (283.15 K). Therefore, homogenous nucleation due to cold air (below the condenser temperature) mixing with the supersaturated vapor can be ruled out.

When deriving the formation rates at 3.2 nm the assumption is made that the CPC detects all particles above its cutoff size and no particles below the d_{50} (step-function approach). In reality the CPC sensitivity is nonzero already at smaller sizes and does not approach unity immediately at the cutoff diameter. Therefore, there were concerns that the step-function approach could result in an erroneous $J_{3.2}$. *Ehrhart et al.* [2016] simulated the two approaches (step-function versus real CPC counting efficiency curve) and found, however, that for most conditions the error made due to the step-function assumption is rather small.

2.3. ACDC Model

The formation of sulfuric acid-ammonia clusters was simulated using the Atmospheric Cluster Dynamics Code (ACDC) [*McGrath et al.*, 2012; *Olenius et al.*, 2013]. The model simulates all possible collision, coagulation, evaporation, and fragmentation reactions, as well as external losses, for a certain set of clusters. Collision and coagulation rates between neutral molecules and clusters are computed directly from kinetic gas theory, while those for ion-neutral collisions are calculated using the parameterization of *Su and Chesnavich* [1982]; for ion-ion recombination a constant value of 1.6×10^{-6} cm^3 s^{-1} is used [*Israël*, 1970]. Evaporation and fragmentation rates are obtained from quantum chemistry [*Ortega et al.*, 2012; *Olenius et al.*, 2013]. In this context fragmentation refers to the evaporation of small clusters from larger clusters, e.g., the fission of a tetramer that can break up into two dimers [*Ortega et al.*, 2012]. The same wall loss parameterization was used as in *Almeida et al.* [2013]; the dilution loss was 9.6×10^{-5} s^{-1}. In the present study we have included neutral, negatively, and positively charged clusters containing up to five sulfuric acid and five ammonia molecules. However, some clusters with an unfavorable acid-base ratio have been left out, as discussed by *Olenius et al.* [2013]. Water molecules and the effect of relative humidity are not taken into account in the simulations.

The steady state formation rate is calculated as the rate of clusters growing larger than the bounds of the simulated system. As these larger clusters are assumed not to evaporate back to smaller sizes, only collisions resulting in clusters with a favorable composition are included in the formation rate. Neutral clusters are allowed to leave the system if they contain at least six acid and five ammonia molecules, negatively charged clusters if they contain at least six acid molecules (including the negative ion) and one ammonia molecule, and positively charged clusters if they contain at least five acid molecules and six ammonia molecules (including the positive ion). Clusters that do not have a favorable composition are brought back to the system by evaporating monomers out of them until they reach the nearest boundary of the simulation system. Note that the formation

rates calculated by ACDC refer to particles with mobility diameters of approximately 1.5 nm. Therefore, the formation rates would be somewhat smaller if they were extrapolated to 1.7 nm, which is the diameter the CLOUD formation rates refer to. However, this attempt was not made since the comparison to the CLOUD data should provide a qualitative picture of the functional dependencies certain parameters have on the NPF.

When simulating cluster formation under GCR or pion beam conditions, ions are introduced via a constant charger ion source term of 3 or 75 ion pairs cm^{-3} s^{-1}, respectively. These generic charger ions, O_2^- and H_3O^+, can then collide with either sulfuric acid or ammonia molecules, or with clusters, thereby transferring their charge. Hydration of the charger ions is neglected although it could potentially affect the number concentration of generated HSO_4^- and NH_4^+ ions by influencing the charging rate of the primary ions. This effect is, however, within the overall uncertainty related to the ion-neutral collision rate parameterization.

The sensitivity of the modeled particle formation rate to uncertainties in cluster formation free energies was studied by increasing or decreasing all formation energies by 1 kcal mol^{-1} and rerunning the simulation. At low temperatures and high sulfuric acid and ammonia concentrations, even the highest evaporation rates were at least slightly lower than the corresponding collision rates, and uncertainties in the quantum chemical cluster energies affected the formation rate relatively weakly. On the other hand, at higher temperatures and lower concentrations, collision rates and some of the rate limiting evaporation rates are of approximately the same order of magnitude, and the net particle formation rate is very sensitive to small variations in cluster formation energies, resulting in larger uncertainties.

2.4. Ammonia Mixing Ratios

An important part of this study is the evaluation of the ammonia mixing ratios during all of the reported experiments. A detailed discussion of the ammonia quantification can be found in Text S1. The experiments can be separated into two different types: (a) experiments with no added ammonia and (b) with ammonia added from a gas bottle through a dedicated stainless steel gas line. Careful characterization and ammonia measurement with different instruments allow the quantification of ammonia when it was added intentionally. However, even the nominally binary runs are not completely free of ammonia, most likely due to wall desorption. In this respect the walls can both act as a sink for ammonia (when it is added to the chamber) and as a source (when no ammonia is added). The ammonia mixing ratios were also estimated under conditions when no ammonia was added. This enables a comparison with the ACDC simulations. In the atmosphere, there is not a sharp transition from pure binary to ternary nucleation, as ammonia mixing ratios span a wide range, including very low values. Therefore, the transition from binary to ternary can only be adequately taken into account if the background ammonia levels are quantified. Nevertheless, under some conditions, e.g., at the lowest temperatures, 208 and 223 K, the influence of contaminant ammonia is believed to be negligible. At these temperatures the APi-TOF mass spectra show no ammonia in the charged clusters under nominally binary conditions [*Duplissy et al.*, 2016]. This indicates that any background ammonia had no significant influence on nucleation. Evidence supporting this statement can be found in *Ehrhart et al.* [2016] and *Duplissy et al.* [2016]. Regarding neutral conditions no ammonia was found in neutral nucleating clusters containing up to 10 sulfuric acid molecules at 208 K [*Kürten et al.*, 2015]. No amines were added to the chamber and a maximum contamination level of 0.1 pptv was estimated by *Schobesberger et al.* [2015] for the CLOUD3 campaign. For the lower temperatures during CLOUD5 and CLOUD7 amines could not be found in the APi-TOF mass spectra at all.

3. Results and Discussion

The results shown here include nucleation rates for the truly binary system [*Duplissy et al.*, 2016], the nominally binary system of sulfuric acid and water (with no added ammonia, but with a potential contribution of ammonia to the particle formation), and the ternary system with the addition of ammonia. In *Duplissy et al.* [2016], a run (experiment) was marked as pure binary based on the APi-TOF measurements. The maximum ratio between the measured concentration of contaminated clusters (containing x sulfuric acid molecules and one ammonia molecule) and the concentration of pure sulfuric acid clusters (containing only x sulfuric acid molecules) was evaluated for $4 \leq x \leq 10$. A threshold of 0.05 for the maximum allowed impurity was selected to discriminate between "pure H_2SO_4-H_2O binary" (ratio smaller than 0.05) and "ammonia contaminated" experiments (ratio larger than 0.05). In this way, all runs at 208 and 223 K were identified as binary as well as some runs at 248 and 278 K. Regarding further discussion about this discrimination we would like to refer the reader to *Duplissy et al.* [2016]. Although the focus of the paper is on the ternary nucleation rates, it is important for

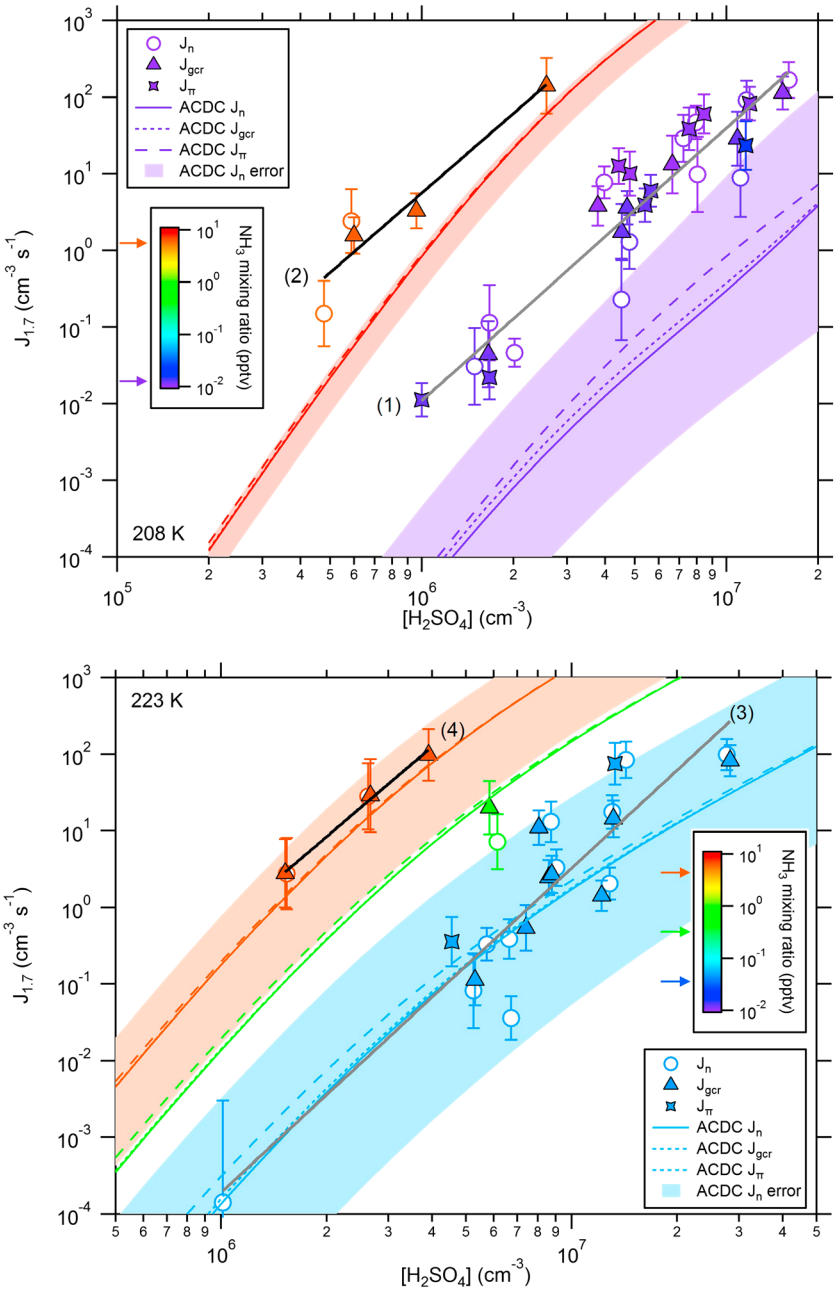

Figure 1. Nucleation rates for neutral (J_n), GCR (J_{GCR}), and pion beam (J_π) conditions as function of the sulfuric acid concentration at chamber temperatures of (top) 208 K and (bottom) 223 K. The color code of the symbols shows the ammonia mixing ratio (arrows next to the legends indicate the NH_3 mixing ratios in the figures). The estimated background ammonia levels are 0.012 pptv for 208 K and 0.05 pptv for 223 K. Results from the ACDC simulations are shown for J_n, J_{GCR}, and J_π. The uncertainty range for ACDC is shown only for the neutral conditions for clarity. The numbered black and grey lines indicate fit curves for which the parameters are provided in Table 2.

the discussion to relate them to the binary system. For temperatures of 248 K and higher, there is evidence that the nominally binary nucleation rates are affected by contaminant ammonia [*Schobesberger et al.*, 2015; *Duplissy et al.*, 2016], which seems to have an especially strong effect on the neutral nucleation rates. This is supported by a comparison between the CLOUD data and nucleation rates calculated from the Sulfuric Acid Water NUCleation model (SAWNUC; [*Ehrhart et al.*, 2016]). We present calculated nucleation rates from the ACDC model for the sulfuric acid-ammonia system and compare them to the measured $J_{1.7}$ for different NH_3 mixing ratios.

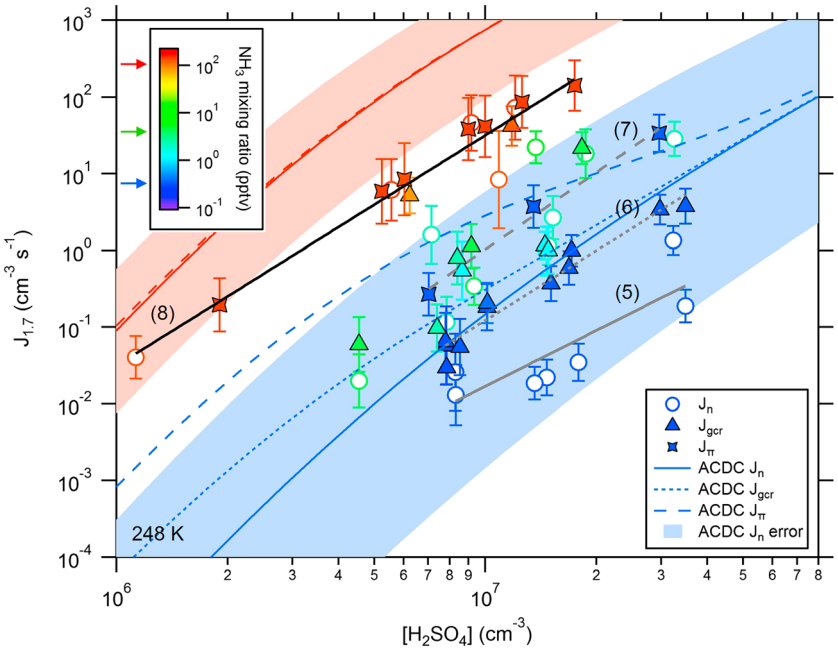

Figure 2. Nucleation rates for neutral (J_n), GCR (J_{GCR}), and pion beam (J_π) conditions as function of the sulfuric acid concentration at a chamber temperature of 248 K. The color code indicates the ammonia mixing ratio (arrows next to the legend indicate the NH_3 mixing ratios in the figure). The nominally binary nucleation rates (blue color) correspond to an estimated contaminant ammonia level of ~0.3 pptv. Results from the ACDC simulations are shown for J_n, J_{GCR}, and J_π. The numbered black and grey lines indicate fit curves for which the parameters are provided in Table 2.

3.1. CLOUD Nucleation Rates Versus Sulfuric Acid Concentration

First we shall discuss the measured data without considering the model results. Subsequently, we shall compare the ACDC model and CLOUD data.

At different chamber temperatures the nucleation rate $J_{1.7}$ was determined for different sulfuric acid concentrations and ammonia mixing ratios. In addition, the nucleation rate was measured under neutral (J_n), galactic cosmic ray (J_{GCR}), or pion beam (J_π) conditions. For most experiments the RH was set to 38%. In some cases, however, the RH varied as well, but no systematic exploration of the RH dependency of J was performed. As mentioned in Text S1 a contaminant ammonia level was assigned to each temperature. Especially for the two lowest temperatures (208 and 223 K) the background ammonia is very low and very likely had no effect on the nominally binary nucleation rates.

Together with the experimental data and the ACDC simulations some fit curves are shown in the Figures 1–4 (black and grey lines). These are not used to derive information about the number of molecules contained in the critical cluster, as it was shown recently that the slope of J versus $[H_2SO_4]$ is strongly influenced by wall loss in chamber or flow tube experiments under certain conditions [*Ehrhart and Curtius*, 2013; *Kupiainen-Määttä et al.*, 2014; *Malila et al.*, 2015]. However, the fit curves serve two purposes: (1) they guide the eye for reading the figures more easily and (2) they are used for normalizing the nucleation rates to a certain sulfuric acid concentration (Text S4). The decision whether a straight-line fit on a log-log plot or a polynomial fit is used was based on the visual impression of the data, although it can be generally said that if only a small range of concentrations is covered, the data can be well represented by a straight-line and if a wider range is covered, a curved shape of the fit curve is better. The parameters for the fits can be found in Table 2, and the numbers in brackets written next to the curves in the figures indicate the corresponding set of values in the table.

3.1.1. Chamber Temperature of 208 K

Figure 1 (top) shows the results for a temperature of 208 K, which was the lowest temperature established in the chamber during CLOUD5 and CLOUD7. The nucleation rates were determined at nominally binary conditions, i.e., without the addition of NH_3. Another set of experiments was carried out at an ammonia mixing ratio of approximately 5 pptv. Clearly, the nucleation rates are strongly enhanced, by about 3 orders

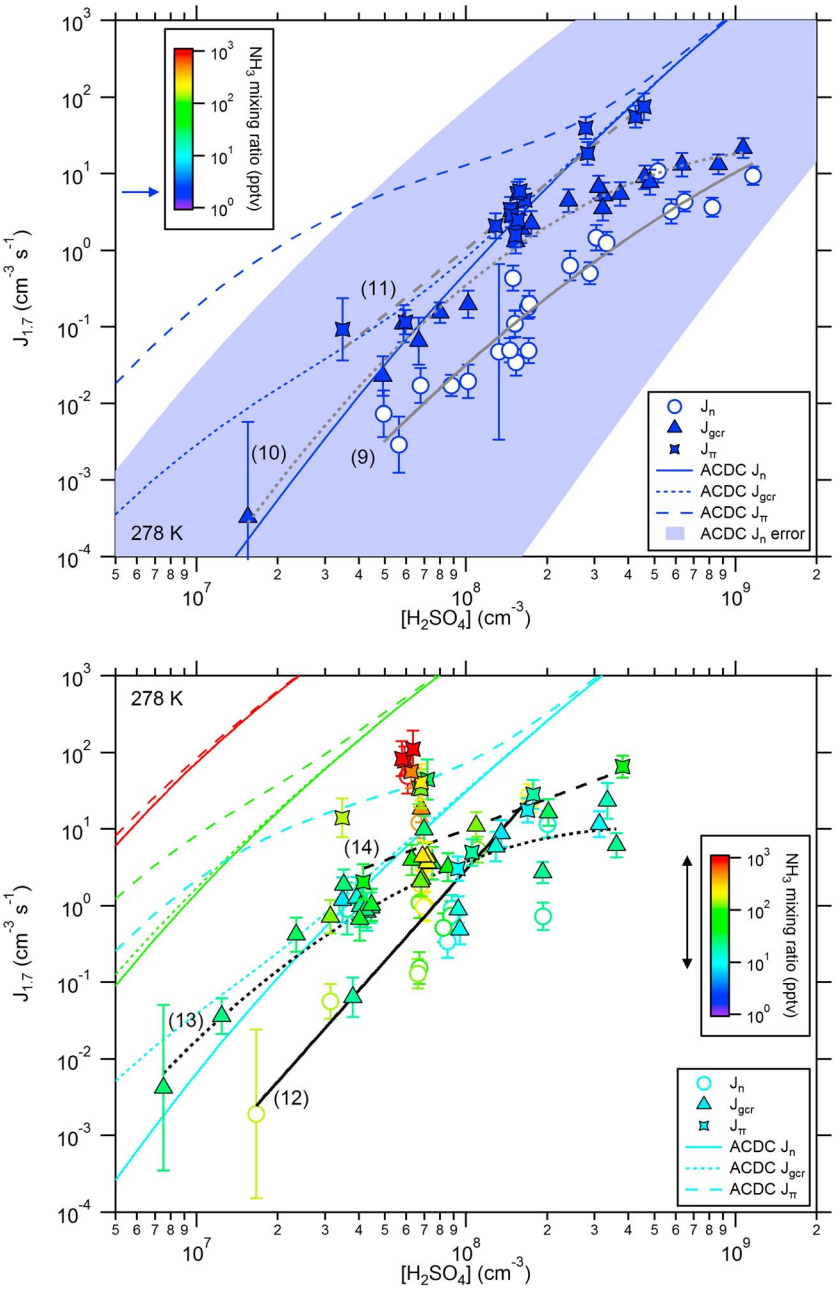

Figure 3. Nucleation rates for neutral (J_n), GCR (J_{GCR}), and pion beam (J_π) conditions as function of the sulfuric acid concentration at a chamber temperature of 278 K. (top) Nucleation rates under nominally binary conditions with an estimated contaminant ammonia level of 2 pptv. (bottom) Nucleation rates when ammonia was added to the chamber. The color code indicates the ammonia mixing ratio (arrows next to the legends indicate the NH_3 mixing ratios in the figures). Results from the ACDC simulations are shown for J_n, J_{GCR}, and J_π while the uncertainty range is only shown for the neutral data with 2 pptv of ammonia (nominally binary in Figure 3, top) for clarity. The numbered black and grey lines indicate fit curves for which the parameters are provided in Table 2.

of magnitude, due to the presence of several pptv of ammonia when the sulfuric acid concentration is ~2×10^6 cm^{-3}. The threshold nucleation rate of 1 cm^{-3} s^{-1}, a value which is sometimes used to define the onset of significant nucleation, is exceeded at a sulfuric acid concentration of ~3×10^6 cm^{-3} for the binary case, and at an acid concentration of ~5×10^5 cm^{-3} for the ternary case with 5 pptv of ammonia. This means that the neutral binary and the neutral ternary NH_3 systems can explain high nucleation rates in the upper troposphere because sulfuric acid concentrations can easily exceed these values [*Mauldin et al.*, 1999].

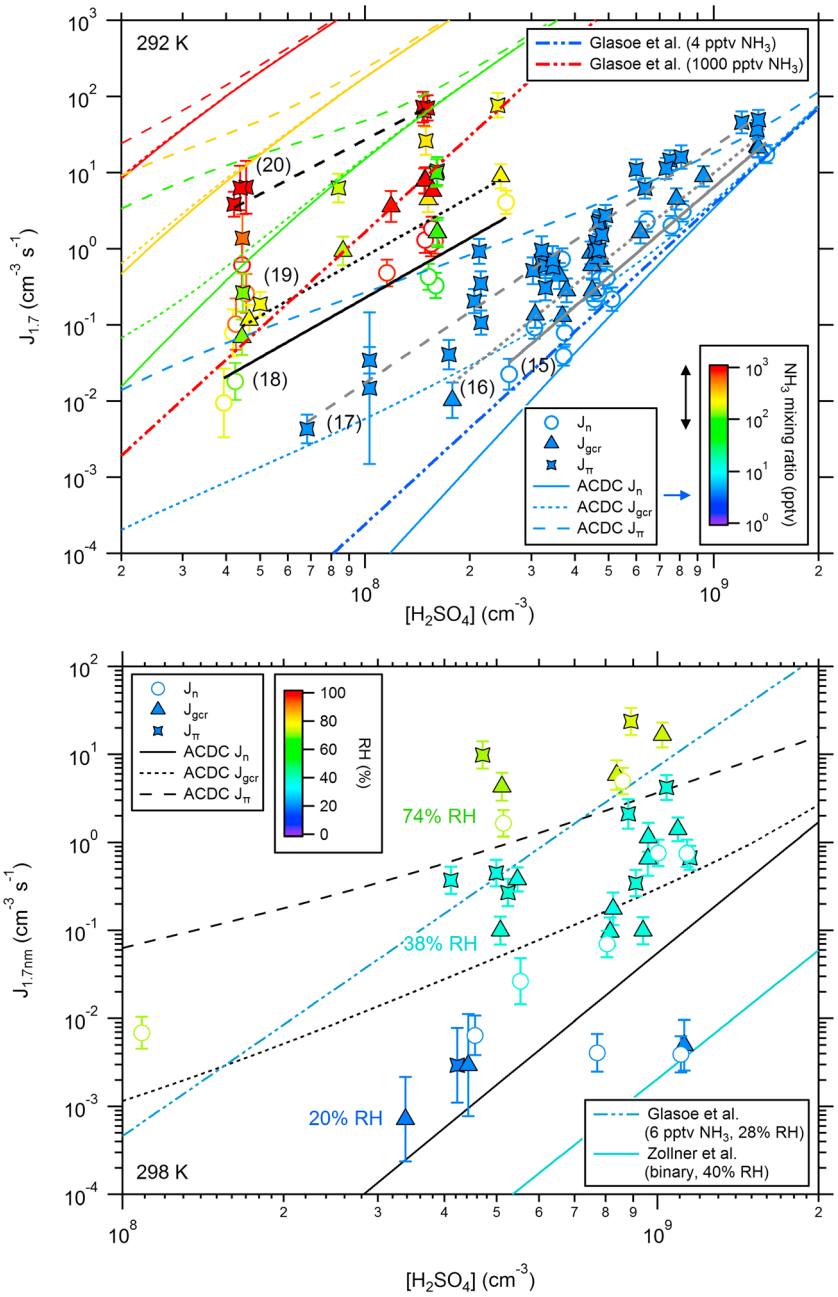

Figure 4. Nucleation rates for neutral (J_n), GCR (J_{GCR}), and pion beam (J_π) conditions as function of the sulfuric acid concentration at chamber temperatures of (top) 292 K and (bottom) 298 K. The color code of the symbols shows the ammonia mixing ratio in Figure 4 (top) (arrows next to the legend indicate the NH_3 mixing ratios in the figure), where the background level is approximately 4.3 pptv. Results from the ACDC simulations are shown for J_n, J_{GCR}, and J_π. In Figure 4 (bottom) the color code represents the relative humidity because ammonia was assumed to be constant at ~6 pptv. The ACDC simulation for an ammonia mixing ratio of 6 pptv (and 0% RH) is shown as well. The numbered black and grey lines indicate fit curves for which the parameters are provided in Table 2. Data from *Glasoe et al.* [2015] and *Zollner et al.* [2012] are shown by the colored straight lines (dash-dotted in Figure 4, top, dash-dotted and solid in Figure 4, bottom).

No significant enhancing effect from ion-induced nucleation is evident for the binary or the ternary system at this low temperature (see section 3.5 and *Ehrhart et al.* [2016]).

3.1.2. Chamber Temperature of 223 K

The experimental data were obtained for acid concentrations between 1×10^6 and 3×10^7 cm^{-3} (Figure 1, bottom). The effect of the addition of ~6 pptv ammonia is very similar to the situation at 208 K. At a sulfuric

Table 2. Functional Relationships Between the Nucleation Rate and the Sulfuric Acid Concentration[a]

Temperature (K)	J versus $[H_2SO_4]$ (no added ammonia)	J versus $[H_2SO_4]$ (with added ammonia)
208	(1) −23.319, 3.559 (J_n, J_{GCR}, J_π)[b]	(2) −19.986, 3.455 (J_n, J_{GCR}, J_π)[b], ~5 pptv of NH_3
223	(3) −29.128, 4.234 (J_n, J_{GCR}, J_π)[b]	(4) −23.604, 3.892 (J_n, J_{GCR}, J_π)[b], ~6 pptv of NH_3
248	(5) −18.715, 2.420 (J_n) (6) −22.078, 3.023 (J_{GCR}) (7) −23.370, 3.340 (J_π)	(8) −19.536, 3.005 (J_n, J_{GCR}, J_π)[b], NH_3 between 50 and 200 pptv
278	(9) −64.395, 12.618, −0.595 (J_n)	(12) −31.174, 3.955 (J_n), NH_3 between 80 and 300 pptv
	(10) −98.736, 21.681, −1.175 (J_{GCR})	(13) −74.376, 17.408, −1.005 (J_{GCR}), NH_3 between 7 and 40 pptv
	(11) −22.792, 2.851 (J_π)	(14) −9.6993, 1.3362 (J_π), NH_3 between 8 and 80 pptv
292	(15) −34.522, 3.925 (J_n)	(18) −21.482, 2.605 (J_n), NH_3 between 70 and 300 pptv
	(16) −32.149, 3.682 (J_{GCR})	(19) −20.854, 2.594 (J_{GCR}), NH_3 between 70 and 300 pptv
	(17) −26.599, 3.104 (J_π)	(20) −17.601, 2.379 (J_π), $NH_3 \geq 300$ pptv

[a]Where two parameters are given, the data are fitted according to $\log(J) = a + b \cdot \log(x)$ (where $x = [H_2SO_4]$; the parameters are given in the order of a and b); three parameters are provided when the data are fitted to a second-order polynomial., i.e., according to $\log(J) = k_0 + k_1 \cdot \log(x) + k_2 \cdot (\log(x))^2$ (order k_0, k_1, and k_2). The numbers in brackets written next to the parameters indicate the labeled fit curves in Figures 1–4. Note that these simple relationships are different from the parameterization used by *Dunne et al.*, [2016] and are only considered to be valid over a narrow range of $[H_2SO_4]$.
[b]Parameters were derived by merging all J values (J_n, J_{GCR}, and J_π).

acid concentration around 4×10^6 cm^{-3}, the enhancement factor compared to binary nucleation reaches a value of ~10^3. Ammonia was added also at ~0.5 pptv, which already significantly increased the nucleation rates. The dependency of J on ammonia is further discussed in section 3.3. Nucleation rates equal to, or larger than 1 cm^{-3} s^{-1}, occur if the acid concentration exceeds 1.5×10^6 cm^{-3} or 8×10^6 cm^{-3}, depending whether ~6 pptv of ammonia or no ammonia is added to the chamber, respectively. Again, since observed sulfuric acid concentrations can reach such concentrations [*Mauldin et al.*, 1999], both the binary and the ternary NH_3 system would, in principle, be capable of explaining nucleation in the upper troposphere or very cold boundary layer regions. The relatively large scatter in the data under nominally binary conditions is not random but related to the fact that different RHs (11, 25, and 50% with respect to supercooled water) were tested at 223 K. Further information about the effect of the RH can be found in *Duplissy et al.* [2016], supporting information Text S3, and Figure S5.

3.1.3. Chamber Temperature of 248 K

At 248 K the nucleation rate depends strongly on the presence of ions for the nominally binary experiments (Figure 2). At $[H_2SO_4] = 10^7$ cm^{-3} the nucleation rates obtained at beam conditions are about 2 orders of magnitude higher than under neutral conditions. Compared to all other conditions, the log-log slope of ~2.4 for the neutral nominally binary nucleation rates is the smallest one observed (see Table 2). Such behavior could be explained by the presence of contaminant NH_3, which stabilizes the neutral clusters and leads to higher nucleation rates than in the pure binary case. If there were a rather constant contaminant ammonia level, then its influence should decrease with increasing $[H_2SO_4]$ because the cluster formation rates would be limited by the availability of NH_3. This assumption is supported by the fact that the APi-TOF detects ammonia in the clusters containing four or more sulfur atoms during the nominally binary charged runs at this temperature [*Schobesberger et al.*, 2015]. The relative abundance of these ammonia-containing clusters decreases with increasing $[H_2SO_4]$, suggesting that the NH_3 contaminant is just at a level where its influence crucially depends on the ratio of the sulfuric acid to the background ammonia. The background level of NH_3 at 248 K has been estimated to be ~0.3 pptv (i.e., ~10^7 cm^{-3}, see the supporting information). If this were indeed the case, then even at an ammonia-to-sulfuric acid concentration ratio of ≤1, the ammonia can have a substantial effect on the neutral nucleation rate at this temperature. In the neutral channel ammonia likely assists in the stabilization of the very small clusters starting with the dimer [*Hanson and Eisele*, 2002]. When the ammonia-to-sulfuric acid ratio decreases due to an increasing acid concentration, the chance that a sulfuric acid dimer will be stabilized by an ammonia molecule before it evaporates decreases.

The contaminant NH_3 does not seem to enhance the ion-induced nucleation rate substantially; this follows from the good agreement of the experimental binary charged nucleation rates with the SAWNUC results [*Ehrhart et al.*, 2016]. As indicated by the APi-TOF data, the larger charged clusters efficiently collect NH_3 molecules, which, however, seem not to lead to any significant enhancement in the formation rates. This would indicate that the charged critical cluster, if it exists at this temperature (see section 3.4), is smaller than the tetramer

because ammonia evaporates rapidly from the smallest charged clusters [*Kirkby et al.*, 2011; *Ortega et al.*, 2014; *Schobesberger et al.*, 2015]. Classical nucleation theory normalized by quantum chemical calculations predicts that ion-induced binary particle formation is kinetic under these conditions, so that it proceeds directly from a collision between the bisulfate ion and the sulfuric acid molecule [*Duplissy et al.*, 2016].

Adding approximately 10 pptv of ammonia increases the nucleation rates substantially over the nominally binary neutral case, leading to similar rates to those for binary ion-induced conditions. Increasing the ammonia level to more than 100 pptv increases the nucleation rates compared with the binary charged and the ternary neutral values at 10 pptv. At NH_3 levels above several pptv, if at all, only a minor enhancement due to charges is evident (see section 3.5).

3.1.4. Chamber Temperature of 278 K

The data obtained for 278 K, shown in Figure 3, exhibit similar behavior as seen at 248 K, discussed above. For sulfuric acid concentrations below 10^9 cm^{-3}, ions substantially enhance the nucleation rates for the nominally binary system (Figure 3, top and also *Kirkby et al.* [2011]). However, in contrast to the data at 248 K, enhancement due to ions is also observed for the ternary NH_3 conditions (Figure 3, bottom). The contaminant background ammonia level has been estimated to be ~2 pptv (i.e., ~5×10^7 cm^{-3}), and the APi-TOF data suggest that ammonia is participating in the nominally binary nucleation [*Schobesberger et al.*, 2015], although the SAWNUC comparison indicates that under pion beam conditions, it has no significant effect [*Ehrhart et al.*, 2016]. Adding NH_3 to the chamber strongly enhances the nucleation rates. This effect will be discussed further below (section 3.3). It is important to note that our results indicate that ternary nucleation involving ammonia could be an important mechanism for nucleation in the polluted boundary layer when temperatures are not too high (i.e., 278 K in this example). At GCR (boundary layer) conditions and an ammonia level of ~100 pptv, a nucleation rate of 1 cm^{-3} s^{-1} is reached at a sulfuric acid concentration of ~4×10^7 cm^{-3}.

3.1.5. Chamber Temperature of 292 K

At 292 K the nominally binary nucleation rates show an enhancement due to the presence of charges (Figure 4, top). However, the enhancement is somewhat smaller than for the temperatures at 248 and 278 K. This could be due to a stronger influence of contaminant ammonia, which could be stabilizing the neutral clusters more strongly than the charged clusters. The addition of ammonia up to a level of ~1400 pptv increases the nucleation rates by orders of magnitude. Again, in strongly polluted areas where ammonia occurs at levels of several hundred pptv, appreciable nucleation can occur below sulfuric acid concentrations of 10^8 cm^{-3}. Therefore, some observed nucleation in polluted areas could, in principle, be explained by the ternary system of H_2SO_4-H_2O-NH_3 and would not necessarily rely on the presence of amines [*Chen et al.*, 2012] or other organic pollutants [*Zhang et al.*, 2004; *Riccobono et al.*, 2014]. However, their presence further increases nucleation rates. Furthermore, evidence exists that synergistic effects between ammonia and amines can be important in atmospheric nucleation [*Yu et al.*, 2012; *Glasoe et al.*, 2015].

3.1.6. Chamber Temperature of 298 K

Results for the warmest temperature studied, 298 K, are shown in Figure 4 (bottom). For those experiments, no ammonia was intentionally added to the chamber, so all experimental data were obtained at the contaminant NH_3 level, estimated to be ~6 pptv (i.e., 1.5×10^8 cm^{-3}). However, three sets of different RH values, i.e., 20%, 38%, and 74%, were studied, respectively. At this temperature the RH seems to have a very strong effect on the neutral and charged nucleation. However, we cannot rule out that this strong influence could also be related to an increase in the ammonia background level that might be correlated with the RH inside the chamber. *Vaittinen et al.* [2014] reported a strong effect of the water concentration on the desorption of ammonia from surfaces. Therefore, the increase in RH could lead to a displacement of ammonia from the chamber walls and lead to an elevated NH_3 background level and consequently to higher nucleation rates. It is interesting to note that the slope of J versus [H_2SO_4] is very flat at the lowest RH of 20%. This could indicate that nucleation is limited with respect to the availability of H_2O or contaminant NH_3. However, the number of data points is quite low, so this cannot be unambiguously shown. Clearly, in future CLOUD studies, the effect of varying RH should be studied in more detail while ensuring that the level of contaminants is insignificant.

3.1.7. Comparison Between CLOUD Data and Previous Studies at 292 and 298 K

Recently, *Glasoe et al.* [2015] investigated the effect of seven bases on the particle formation rate for the system of sulfuric acid and water (plus the added base). Among the different bases the addition of ammonia was also

tested in flow tube experiments. Regarding the formation rate of particles (larger than ~1.8 nm in mobility diameter) the following equation was reported [*Glasoe et al.*, 2015]:

$$J\left(\mathrm{cm^{-3}s^{-1}}\right) = 10^{-50} \cdot [\mathrm{H_2SO_4}]^{4.2} \cdot [\mathrm{NH_3}]^{1.6}, \quad (1)$$

where the concentrations of sulfuric acid and ammonia are used in units of $\mathrm{cm^{-3}}$. The equation is derived from data measured at a temperature between 296 and 300 K and at a relative humidity of 28%. For the conditions of the flow tube study with relatively high sulfuric acid concentrations ($> \sim 2 \times 10^9\ \mathrm{cm^{-3}}$) we assume that the particle formation was mainly due to neutral conditions. Figure 4 (top) includes two curves calculated from equation (1) by using ammonia mixing ratios of 4.3 pptv (estimated contaminant level of ammonia at 292 K; Figure 4, dash-dotted blue line) and 1000 pptv (Figure 4, dash-dotted red line). Both lines show relatively good agreement with the CLOUD data, especially for the nominally binary conditions with an estimated ammonia level of 4.3 pptv. Regarding this estimation the comparison between data from this study and from *Glasoe et al.* [2015] indicates that our reported ammonia background should be quite accurate. For higher NH_3 mixing ratio the agreement is also quite good, which is discussed further below (section 3.3.3).

The data at 298 K (Figure 4, bottom) are also compared to equation (1) for an estimated ammonia background level of 6 pptv (Figure 4, dash-dotted cyan line). Equation (1) is derived for conditions of 28% RH; the agreement with the CLOUD data for an RH of 38% (cyan data points) is relatively good.

Another study reports binary nucleation rates from the same flow tube [*Zollner et al.*, 2012]. We have used the data from *Zollner et al.* [2012] to derive an expression for the particle formation rate at an RH of 40% and a temperature of 296 to 300 K:

$$J\left(\mathrm{cm^{-3}s^{-1}}\right) = 10^{-46.33} \cdot [\mathrm{H_2SO_4}]^{4.85}. \quad (2)$$

The sulfuric acid concentrations from *Zollner et al.* [2012] were between 2×10^9 and $1 \times 10^{10}\ \mathrm{cm^{-3}}$, therefore using equation (2) in Figure 4 (bottom) extrapolates their conditions to lower sulfuric acid (solid cyan line). These formation rates are lower by up to 3 orders of magnitude compared to the data from our study (cyan symbols), indicating that contaminant ammonia did indeed play a role at these warm temperatures. This is also confirmed by the good agreement between equation (1) and our data when using the estimated background ammonia level (see above).

3.2. ACDC Nucleation Rates Versus Sulfuric Acid Concentration

3.2.1. Chamber Temperature of 208 K

The calculated nucleation rates from the ACDC model for an ammonia mixing ratio of 5 pptv are in good agreement with the experimental data (Figure 1, top). The simulated nucleation rates for the nominally binary runs are about a factor of 100 lower than the measured values. For this simulation, 0.012 pptv of ammonia was assumed, which is the estimated background ammonia mixing ratio (see Text S1). However, the nucleation rates under these conditions are unlikely to be strongly influenced by the ternary system with ammonia but are more likely pure binary as shown elsewhere [*Duplissy et al.*, 2016; *Kürten et al.*, 2015; *Ehrhart et al.*, 2016]. Therefore, only sulfuric acid and water vapor participate in the cluster formation. Since water vapor is not included in the ACDC simulations presented here, this underestimation of the formation rates is reasonable. The simulations predict only a minor enhancement in J for GCR and pion beam conditions, which is in qualitative agreement with the CLOUD data.

3.2.2. Chamber Temperature of 223 K

The ACDC simulations agree well with the experimental data for the simulated ammonia mixing ratios of 0.05, 0.5, and 6 pptv shown in Figure 1 (bottom). As stated above, the ACDC simulations do not include water, so the good agreement at the background ammonia level could indicate that 0.05 pptv of ammonia has a similar effect on the nucleation rates in ACDC as 38% RH has on the experimental nucleation rates. There is good agreement between the CLOUD data showing the absence of ammonia in sulfuric acid clusters with predictions from the SAWNUC model [*Ehrhart et al.*, 2016] and classical nucleation theory normalized by quantum chemical calculations [*Duplissy et al.*, 2016]. The predicted enhancement in J due to charges is minor.

3.2.3. Chamber Temperature of 248 K

The agreement between ACDC and the measured nucleation rates is not as good at 248 K as it is for the lower temperatures (Figure 2). Over the range of sulfuric acid concentrations studied for the nominally binary neutral runs (i.e., at a background ammonia level of ~0.3 pptv), the ACDC prediction yields about a factor of 5 to 100 higher

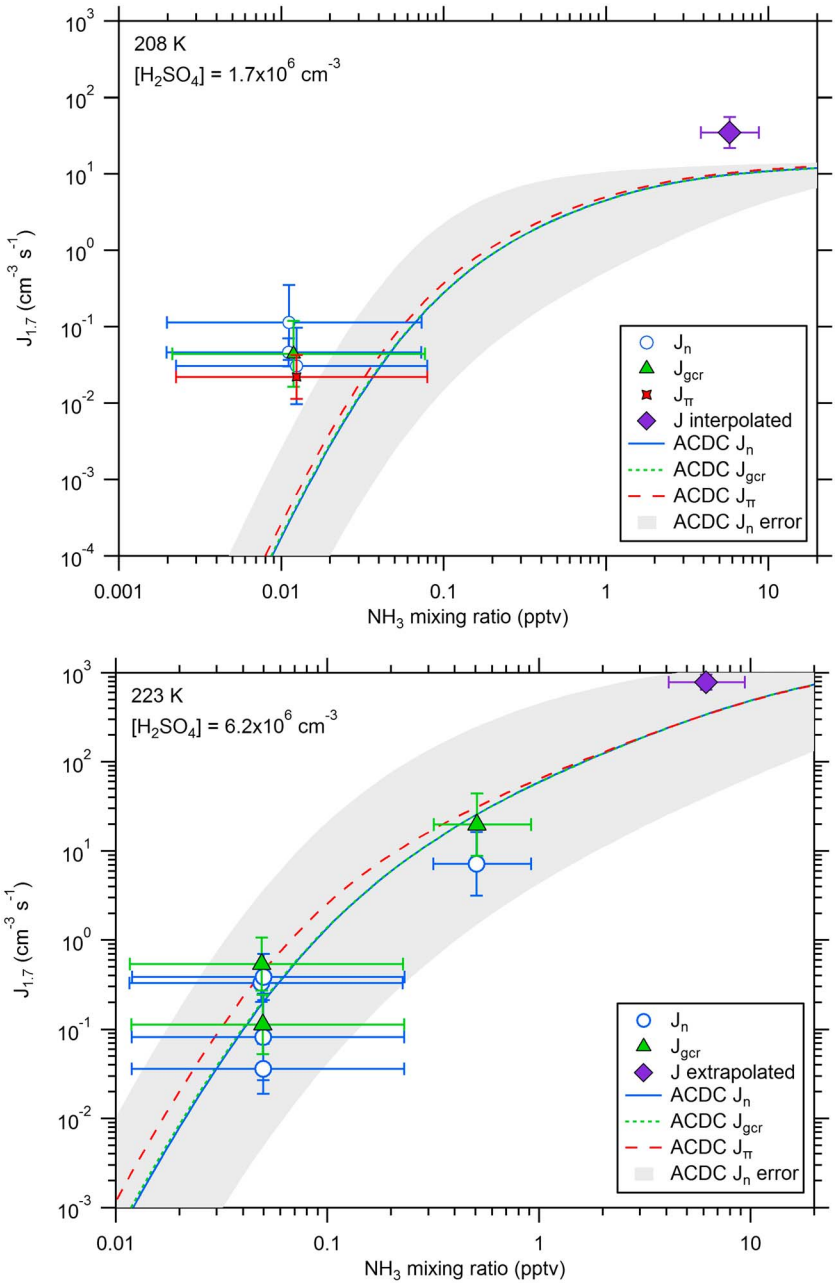

Figure 5. Nucleation rates as function of the ammonia mixing ratio. The $[H_2SO_4]$ is (top) 1.7×10^6 cm^{-3} for 208 K and (bottom) 6.2×10^6 cm^{-3} for 223 K. The diamond symbols do not represent directly measured nucleation rates. Instead, their values were calculated from the parameters shown in Table 2 (parameter set (2) for 208 K and (4) for 223 K). The colored lines represent the nucleation rates calculated using ACDC for neutral, GCR, and pion beam conditions.

nucleation rates with a slightly steeper slope. For GCR and pion beam conditions (at 0.3 pptv of ammonia), there is on average a slight over-prediction by the model. In addition, ACDC underpredicts the enhancement by GCR compared to neutral conditions. The simulated nucleation rates at 140 pptv of ammonia show a slightly steeper slope as a function of the sulfuric acid concentration than the measurements; this results in an overestimation of a factor of ~50 at $[H_2SO_4] = 1 \times 10^7$ cm^{-3}. At this high ammonia concentration no significant enhancement in the nucleation rate from ions is predicted. Despite the increasing discrepancy between ACDC and the experimental data, the agreement is still quite good, and the functional behavior of the experimental data is well represented by the model. However, one should note that the uncertainty range spans 3 to 4 orders of magnitude for the nominally binary neutral simulation.

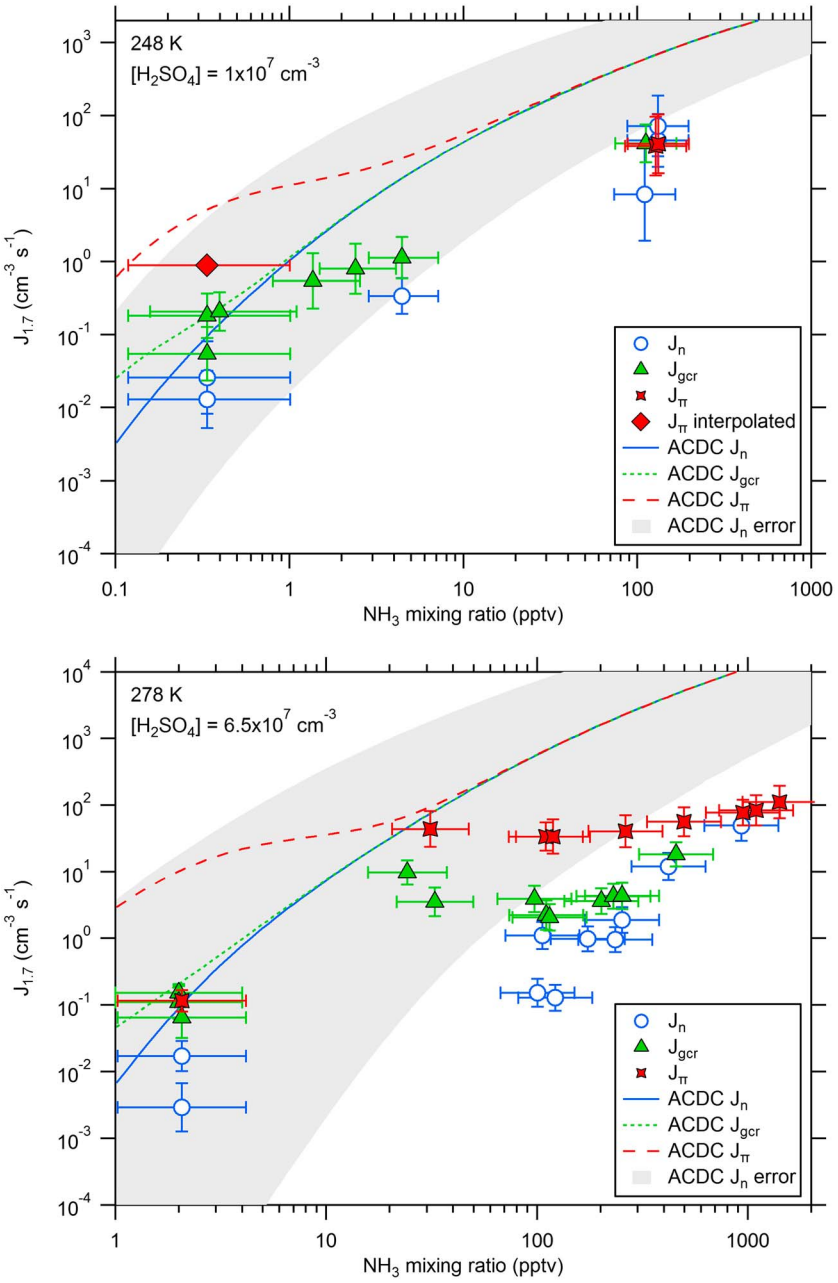

Figure 6. Nucleation rates as function of the ammonia mixing ratio. The $[H_2SO_4]$ is (top) 1×10^7 cm^{-3} for 248 K and (bottom) 6.5×10^7 cm^{-3} for 278 K. The diamond symbol does not represent directly measured nucleation rates. Instead, its value was calculated from the parameters shown in Table 2 (parameter set (7) for 248 K). The colored lines represent the nucleation rates calculated using ACDC for neutral, GCR, and pion beam conditions.

3.2.4. Chamber Temperature of 278 K

The nucleation rates calculated by ACDC for 278 K (Figure 3) show similar behavior to that for 248 K. Under nominally pure binary conditions, i.e., at approximately 2 pptv of ammonia, the simulated neutral nucleation rates are a factor 10 to 200 higher than the measured ones over a range of 5×10^7 to 1×10^9 cm^{-3} in $[H_2SO_4]$ (Figure 3, top). The larger deviation occurs at the higher sulfuric acid concentrations. Moreover, the slope of the calculated *J* values is somewhat higher than the experimentally determined slope (Table 2). For GCR and pion beam conditions at 2 pptv of ammonia, the agreement is quite good at the higher acid concentrations, but below 1×10^8 cm^{-3}, the discrepancy increases. For the higher ammonia levels the disagreement between ACDC and the experiment becomes very pronounced, meaning that ACDC is overpredicting the

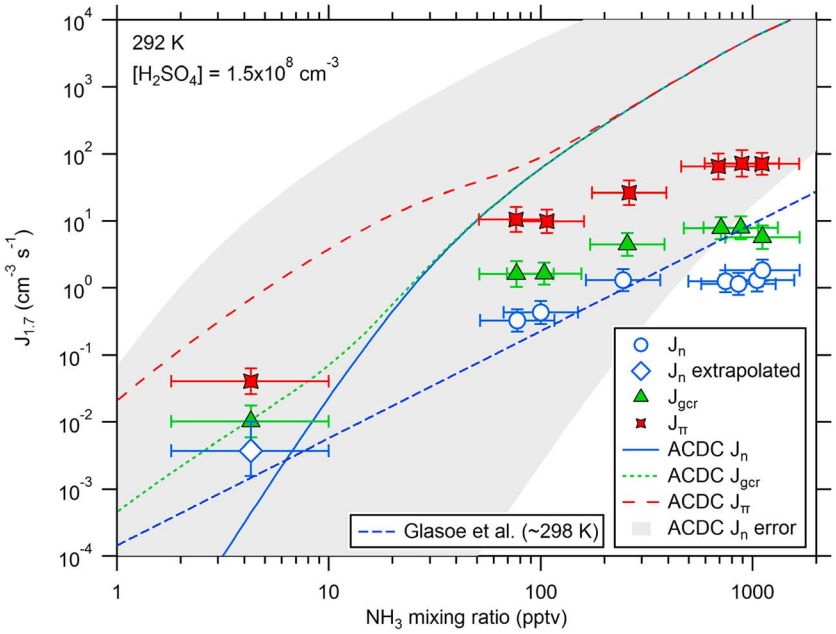

Figure 7. Nucleation rates as function of the ammonia mixing ratio for a temperature of 292 K. The $[H_2SO_4]$ is 1.5×10^8 cm^{-3}. The diamond symbol does not represent directly measured nucleation rates. Instead, its value was calculated from the parameters shown in Table 2 (parameter set (15)). The colored lines show the nucleation rates calculated using ACDC for neutral, GCR, and pion beam conditions. Data from *Glasoe et al.* [2015] are shown by the dashed blue line.

nucleation rates. The discrepancy reaches up to about 4 orders of magnitude due to a stronger dependence on NH_3 compared to the measurements (Figure 3, bottom). Due to the high sensitivity of the calculated nucleation rates on the cluster evaporation rates, the ACDC uncertainty ranges become large for the warmer temperatures covering many orders of magnitude. For clarity only the uncertainty for the nominally binary neutral nucleation is shown.

3.2.5. Chamber Temperature of 292 K

The ACDC predictions show a good agreement with the measured nucleation rates for background ammonia conditions (Figure 4, top). This is somewhat surprising because for the temperatures of 248 and 278 K the disagreement was significant. Due to the high uncertainty of the model calculations (see below) the agreement could be coincidental. Only in the ion-induced channel does ACDC overpredict the nucleation rates at the lower sulfuric acid concentrations. For the higher ammonia mixing ratios the simulated nucleation rates are up to about 4 orders of magnitude higher than the measured ones (neutral conditions at ~1000 pptv of ammonia). Again, it has to be noted here that the ACDC predictions include very high uncertainties covering many orders of magnitude (e.g., 9 orders of magnitude at 5×10^8 cm^{-3} of sulfuric acid for neutral nominally binary conditions). Because the uncertainty range would cover the whole figure it has been neglected in Figure 4.

3.2.6. Chamber Temperature of 298 K

The varying relative humidities at 298 K had a strong influence on the nucleation rates. Since the effect of water vapor is not considered in the simulations the predicted and measured nucleation rates cannot be directly compared (Figure 4, bottom). Clearly, the effect of RH needs to be further studied both experimentally and by quantum chemical calculations [e.g., *Henschel et al.,* 2014]. Model studies using thermochemical data from measurements investigating the binary nucleation of sulfuric acid and water can be found elsewhere [*Panta et al.*, 2012; *Ehrhart et al.*, 2016].

3.3. Nucleation Rates as Function of the Ammonia Mixing Ratios

The dependence of the nucleation rates on the ammonia mixing ratios is shown in Figures 5–7 and Figures S6–S8. For each temperature the formation rates within a narrow range (±25%) of $[H_2SO_4]$ were identified; the midpoints of these ranges are 1.7×10^6 cm^{-3} (208 K), 6.2×10^6 cm^{-3} (223 K), 1×10^7 cm^{-3} (248 K), 6.5×10^7 cm^{-3} (278 K), and 1.5×10^8 cm^{-3} (292 K). Because the data coverage is sparse for some temperatures and conditions (regarding the sulfuric acid concentration and the ammonia mixing ratio), interpolation or

extrapolation was applied to estimate representative values from the functions and parameters provided in Table 2. It has to be noted that the expressions from Table 2 are not meant to be indicative for the nucleation processes. Instead, they provide an easy way to summarize the data for certain conditions.

In addition to the directly measured nucleation rates (and the few data points from the extrapolation/interpolation), additional analysis was performed by normalizing all J values for one temperature to a certain sulfuric acid concentration (see Text S4). Although this has the advantage that more data points are available (thereby improving the statistical significance), the method involves the uncertainty regarding the fit parameters, which are only derived for a subset of the data over a rather narrow range of the ammonia mixing ratios. Nevertheless, the two different methods (Figures 5–7 and Figures S6 to S8) show very similar results.

The experimental data were compared to model results from ACDC for neutral, GCR, and pion beam conditions.

3.3.1. Chamber Temperatures of 208 and 223 K

For the two lowest temperatures, 208 and 223 K, ACDC and the experimental results agree rather well (Figures 5 and S6). The data at the highest ammonia mixing ratios were obtained by interpolating (extrapolating) the fit curve from Figure 1 (top) (Figure 1, bottom) for 208 K (223 K) to 1.7×10^6 cm^{-3} (6.2×10^6 cm^{-3}). For pure binary conditions (at contaminant NH_3 level), the experimental data agree within error bars with the ACDC curves. However, as mentioned above, the simulations do not account for the effect of water vapor. Therefore, the good agreement for the very low ammonia mixing ratios is likely for the wrong reason. The existence of water in the experiment seems to have an effect that is comparable to that of ammonia in the ACDC simulations. This is, however, speculative because the background NH_3 levels are not known accurately. At 208 K and a NH_3 mixing ratio above several pptv, the simulated nucleation rates reach a plateau (Figure 5, top). At this temperature, ACDC modestly underestimates the measured nucleation rates. The fact that the simulated nucleation rates approach a plateau indicates that the new particle formation is limited by the availability of sulfuric acid. At 223 K the addition of less than 1 pptv of ammonia leads to an enhancement in J of a factor ~100 (Figure 5, bottom), although one has to note that the uncertainty in the NH_3 mixing ratio is quite large. At an even higher ammonia level of ~6 pptv, the enhancement factor compared to the pure binary system reaches a value of >1000, which demonstrates the very strong effect of small amounts of NH_3 at these temperatures and low acid concentrations.

3.3.2. Chamber Temperatures of 248 and 278 K

In Figures 6 and S7 the results are shown for temperatures of 248 and 278 K. For both temperatures the ACDC simulations overestimate the nucleation rates for the high NH_3 mixing ratios. This overestimation could be due to an overestimation in the cluster stability. The addition of ~100 pptv of ammonia at 248 K enhances J by about 3 orders of magnitude compared to the nominally binary system for neutral conditions (Figure 6, top). Here it is important to remember that even the nominally binary neutral runs are very likely affected by contaminant NH_3. For the nominally binary experiments a clear charge effect can be observed. The formation rate under beam and nominally binary conditions was obtained from the fit parameters shown in Table 2 since no directly measured formation rates are available at an acid concentration of 1×10^7 cm^{-3}. The charge enhancement seems to decrease substantially for the high NH_3 levels (section 3.5). The enhancement in J due to the addition of ammonia is similar for 278 K (Figure 6, bottom), but here the charge effect is pronounced even at several hundred pptv of ammonia, which is not reflected by the ACDC simulations. Eventually, the charge effect decreases because the nucleation rates reach values that are close to the ionization rate; the ion-induced nucleation rates saturate. However, there are only a few data points at the high ammonia mixing ratios. The charge effect will be further discussed in section 3.5.

3.3.3. Chamber Temperature of 292 K

In Figures 7 and S8 the dependence of J on the ammonia mixing ratio is shown for 292 K. The nucleation rate is again a strong function of the ammonia mixing ratio. At the lowest ammonia levels the charge enhancement is pronounced; it is even somewhat higher at the higher NH_3 mixing ratios. No clear saturation effect is visible for the ion-induced nucleation pathway in contrast to 278 K. As in the simulation at 278 K, ACDC does not predict a significant charge enhancement once the ammonia level exceeds a certain threshold. This can be interpreted such that the neutral cluster evaporation rates are underestimated.

The data by *Glasoe et al.* [2015] are included in Figure 7 (dashed blue line) by using a constant sulfuric acid concentration of 1.5×10^8 cm^{-3} in equation (1). For most ammonia mixing ratios the agreement with the CLOUD data is very good, except for the highest ammonia mixing ratios where the CLOUD data yield formation rates

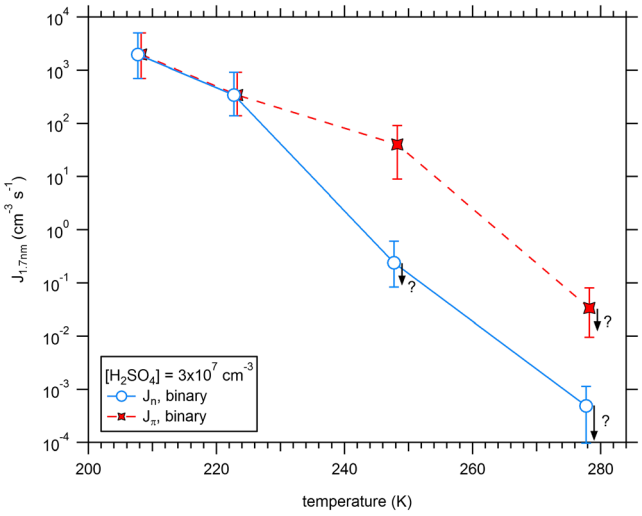

Figure 8. Nucleation rates as a function of chamber temperature for a sulfuric acid concentration of 3×10^7 cm^{-3}. The values were determined according to the relationships shown in Table 2. Note that the data points marked with an arrow at 248 and 278 K are likely lower for the "true" binary case because under these conditions signs of an influence by contaminant ammonia were found. Data points are slightly offset from their position on the *x* axis for improved readability and lines are provided to guide the eye.

that are about 1 order of magnitude lower than the ones from *Glasoe et al.* [2015]. However, it has also to be noted that the temperatures for the two experiments are slightly different (292 K in CLOUD and ~298 K for *Glasoe et al.* [2015]). Since an increasing temperature has the tendency to lower particle formation rates the comparison is more of a qualitative nature.

3.4. Nucleation Rate Versus Temperature

The temperature dependence of *J* between 208 and 278 K at otherwise constant nominally binary conditions is shown in Figure 8. Given that the measurable nucleation rates at CLOUD span approximately a range from 10^{-4} to 10^3 cm^{-3} s^{-1}, and that *J* varies strongly with *T* and [H_2SO_4], only a narrow range of sulfuric acid concentrations covers different temperatures for which nucleation rates were measured. A sulfuric acid concentration of 3×10^7 cm^{-3} was chosen to compare the nominally binary nucleation rates under neutral and pion beam conditions. However, for the two lowest temperatures of 208 and 223 K, the maximum established [H_2SO_4] were 1.5×10^7 cm^{-3} and 2.8×10^7 cm^{-3}, respectively. For the highest temperature (278 K) the lowest established [H_2SO_4] were 4.9×10^7 cm^{-3} (neutral conditions) and 3.5×10^7 cm^{-3} (pion beam conditions), respectively. For this reason some nucleation rates were extrapolated in order to obtain values at 3×10^7 cm^{-3}. The functional relationships given in Table 2 were used to calculate the nucleation rates at the four different temperatures. Extrapolating a nucleation rate bears some risk, but since the differences between the measured [H_2SO_4] range and the concentration where the nucleation rates are extrapolated to are small (at maximum a factor of 2), it is assumed that the errors stay in a reasonable range.

At the two lowest temperatures (208 and 223 K), no clear difference could be observed between neutral and pion beam conditions. Since the ionization rate is ~75 ion pairs cm^{-3} s^{-1}, and the nucleation rates at the two lowest temperatures clearly exceed this value, the preferred nucleation pathway has to be the neutral one under these conditions [*Ehrhart et al.*, 2016]. However, at 248 K a very pronounced charge enhancement is observed. The nucleation rate under pion beam conditions is about 2 orders of magnitude higher than the neutral nucleation, even though the neutral nucleation rate is probably more strongly affected by contaminant ammonia. This indicates that the ion-induced nucleation mechanism is very efficient. At 278 K the nominally binary data are very likely biased toward higher values due to the presence of contaminant ammonia. Nevertheless, the ion-induced pathway yields a nucleation rate that is about a factor of 100 higher than the neutral nucleation. At this temperature we cannot rule out that even the charged nucleation is influenced by contaminant ammonia, although the effect is probably small [*Duplissy et al.*, 2016; *Ehrhart et al.*, 2016].

It is important to note that the ion-induced nucleation rates include a contribution from the neutral channel. Therefore, the charged channel becomes almost negligible for the very low temperature of 208 K although ion-induced nucleation is proposed to be barrierless already at temperatures below approximately 250 K (for RH ~40% and [H_2SO_4] = 1×10^7 cm^{-3} [*Lovejoy et al.*, 2004]). The neutral nucleation pathway dominates at the lower temperatures because of the strong decrease of the cluster evaporation rates [*Kürten et al.*, 2015; *Schobesberger et al.*, 2015]. Even if the charged clusters have lower evaporation rates than neutral clusters, their formation rate is limited by the ionization rate and the resulting low ion concentrations [*Raes and Janssens*, 1985; *Lovejoy et al.*, 2004; *Hanson and Lovejoy*, 2006]. Therefore, neutral nucleation will always dominate at low temperature, i.e., when evaporation rates are low, or when sulfuric acid concentrations are high. Even

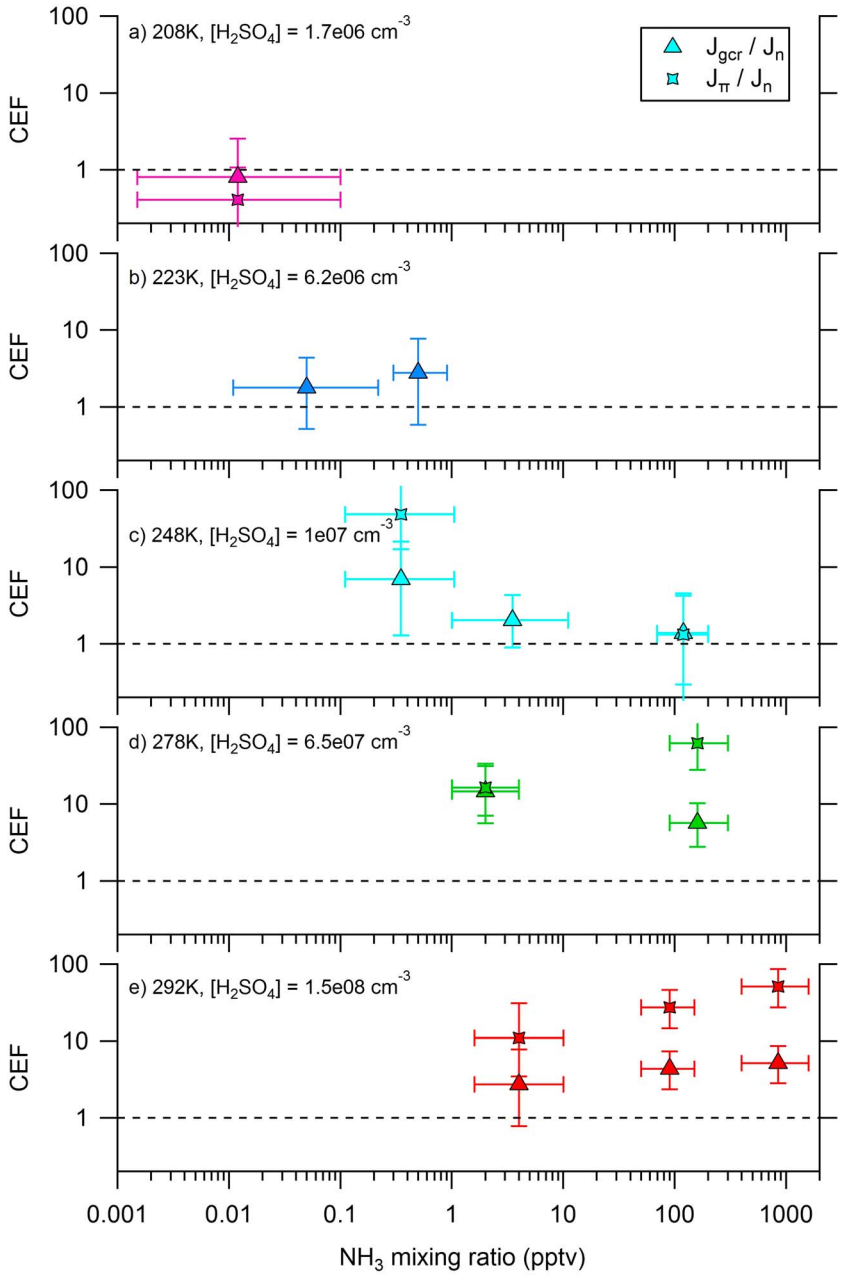

Figure 9. Charge enhancement factors (CEF) as a function of the ammonia mixing ratio for different temperatures: (a) 208 K, (b) 223 K, (c) 248 K, (d) 278 K, and (e) 292 K. Charge enhancement factors J_{IIN}/J_n are shown for GCR (triangles) and pion beam conditions (stars).

though very stable clusters can be formed in the case of ion-induced nucleation at low temperature, particle formation rates can still be lower than the ion pair production rate because of losses (e.g., wall loss and ion-ion recombination), which are especially important when particle growth is slow [*Ehrhart and Curtius*, 2013]. If ammonia is added to the system, the neutral cluster evaporation rates will be even lower compared to the binary case [*Kürten et al.*, 2015], making the charge effect even smaller.

3.5. Charge Enhancement Factors

The presence of charges generally enhances the nucleation rate for the truly binary system (with higher enhancement at higher temperature) [*Duplissy et al.*, 2016; *Ehrhart et al.*, 2016] and for the nominally binary and the ternary system involving ammonia [*Kirkby et al.*, 2011]. Figure 9 shows the charge enhancement

factor (CEF), i.e., the ratio of J_{IIN} to J_n, where the ion-induced nucleation rate J_{IIN} is either J_{GCR} or J_{π}, respectively. The charge enhancement factors have been evaluated for the different temperatures. In addition, for calculating these factors, the data were segregated with respect to certain ranges of ammonia levels. These ranges are indicated for each data point by the horizontal bars, and CEF are plotted against the mean ammonia level where the lowest level always indicates the nominally binary data for each temperature. The bars in the vertical direction indicate the error of the ratio calculated from the mean uncertainties of J_{IIN} and J_n.

It is important to note that the calculated enhancement factors depend also on the sulfuric acid concentration. In general, when going to high sulfuric acid concentrations, the neutral nucleation rates will eventually exceed the ion pair production rate; as a result, the charge enhancement factors approach unity. Therefore, the values shown in Figure 9 provide a snapshot of the charge effect at the indicated conditions. If one wants to take into account also the influence of [H_2SO_4] the full parameterization of the data should be used [*Dunne et al.*, 2016].

At 208 K there is no sign that the presence of charges significantly increases the nucleation rates at a sulfuric acid concentration of $[H_2SO_4] = 1.7 \times 10^6$ cm^{-3}. Considering the error bars, the enhancement under GCR conditions at 223 K is not very significant. This is supported if one takes into account that the data point at ~0.5 pptv is a result of only two nucleation experiments (one under neutral and one under GCR conditions) and has therefore only a weak statistical significance. At 248 K the charge enhancement factor reaches a value of ~50 under pion beam conditions and a value of ~7 under GCR conditions. The slight charge enhancement seen for ammonia mixing ratios of several pptv (CEF of ~2 in Figure 9 at ~3.5 pptv of NH_3) is not significant because only one neutral experiment is taken into account. The charge enhancement even disappears when taking into account more data points due to the normalization (Figure S7, top). On the other hand, even lower levels than the estimated background of 0.3 pptv could lead to even bigger enhancement factors because it seems likely that the neutral nucleation rates under nominally binary conditions are more strongly affected by contaminant ammonia than the ion-induced nucleation rates. A very strong charge enhancement under these conditions is also seen in the SAWNUC calculations [*Ehrhart et al.*, 2016]. At 278 K the presence of charges leads to an increase in the nucleation rates, which seems to be almost independent of ammonia over the investigated range. The value of the CEF spans a range from 5.6 (GCR conditions at highest ammonia level) to 62 (pion beam conditions at highest ammonia levels). At 292 K the situation is similar to the one at 278 K. The ion-induced nucleation rates under pion beam (GCR) conditions are a factor 11 to 51 (3 to 5) higher than the neutral ones.

In summary, the data show that ion-induced nucleation is not very important at low temperatures. When going to 248 K, ion-induced nucleation is significantly more efficient than neutral nucleation when ammonia levels are low. However, at elevated ammonia mixing ratios the enhancement due to ions disappears because in the neutral nucleation pathway ammonia molecules can efficiently stabilize the clusters. The neutral cluster concentrations overwhelm the charged cluster concentrations where ammonia does not have an effect on the smallest sizes because it rapidly evaporates until at least four sulfuric acid molecules (including the bisulfate ion) are present in the cluster [*Olenius et al.*, 2013; *Schobesberger et al.*, 2015]. At even higher temperatures (278 and 292 K) the presence of charges increases the nucleation rates also at high ammonia mixing ratios. This indicates that despite the fact that ammonia stabilizes the neutral clusters, their evaporation rates are still rather high, and therefore, ion-induced nucleation can compete with and even overwhelm neutral particle formation.

4. Summary and Conclusions

More than 300 individual particle formation rates at a mobility diameter of 1.7 nm were presented from measurements at the CLOUD chamber. Different temperatures between 208 and 298 K were adjusted probing a range of sulfuric acid concentrations and ammonia mixing ratios. Furthermore, the effect of ion-induced nucleation was extensively studied by either eliminating the effect of ions through the use of a high-voltage clearing field (neutral conditions) or by allowing ions from galactic cosmic rays (GCR conditions) or a pion beam (pion beam conditions) from the CERN proton synchrotron to participate in the formation of new particles. The data set is used to derive a parameterization, which is presented elsewhere [*Dunne et al.*, 2016]. The parameterized particle formation rates are implemented into the GLObal Model of Aerosol Processes [*Dunne et al.*, 2016].

The data show that nucleation rates strongly decrease with increasing temperature. Both ions and ammonia have an enhancing effect on the nucleation rates [*Kirkby et al.*, 2011; *Zollner et al.*, 2012; *Glasoe et al.*, 2015]. At low temperatures (208 and 223 K) when the neutral clusters are already pretty stable and the sulfuric acid concentration is not too low, charges do not have a significant effect on nucleation. However, when ammonia is present in the pptv range, it enhances the nucleation rates significantly. At higher temperatures (248 K) ions have a strong effect on the binary system (because the neutral cluster evaporation rates are significant), but not on the ternary system because the more abundant ammonia molecules stabilize the clusters very efficiently. At even higher temperatures (278 and 292 K), both the binary and the ternary system show elevated nucleation rates under the presence of ions because the neutral cluster evaporation rates are high and therefore the addition of charge efficiently stabilizes the clusters.

Regarding the importance of ion-induced nucleation, we want to emphasize that the CLOUD data suggest where this effect should be most important. At 248 K and the lowest ammonia levels (i.e., under nominally binary conditions) the enhancement in the nucleation rates due to the presence of charges is high, while nucleation is efficient at the same time due to the rather low temperature. Consequently, in clean upper tropospheric regions where ionization rates are high and the levels of ternary substances are low, the ion-induced nucleation pathway could be dominant [*Lee et al.*, 2003; *Lovejoy et al.*, 2004].

Neutral and ion-induced nucleation rates were also calculated with the Atmospheric Cluster Dynamics Code (ACDC) and evaporation rates calculated by quantum chemistry. The nucleation rates were calculated for different levels of sulfuric acid and ammonia. The effect of water vapor was not taken into account; therefore, it is unreasonable to expect the simulations to reliably predict the formation rates for conditions when the ammonia levels are low and binary nucleation is the preferred pathway. Given this limitation, the formation rates at the two lowest temperatures (208 and 223 K) agree with the simulations within the uncertainties. Other model approaches, using, e.g., thermochemical data from experiments for binary nucleation could be used for such conditions [*Panta et al.*, 2012; *Ehrhart et al.*, 2016]. The formation rates in the ternary system at 248 K also agree quite well (1 to 2 orders of magnitude deviation between measurements and simulations). However, for the warmer temperatures the deviation between the modeled and the measured data becomes larger reaching many orders of magnitude. This suggests that the quantum chemical data used overestimate the binding of the clusters. Because of the exponential dependence of evaporation rates on cluster formation energies, even small uncertainties in the cluster formation energies translate to big changes in the formation rates. Nevertheless, generally the simulated and measured formation rates show a very similar trend as a function of the sulfuric acid concentration and the ammonia mixing ratio.

Chen et al. [2012] suggested that nucleation in polluted areas can be explained by the system involving sulfuric acid, water, and ammonia or amines. This study, in principle, confirms that nucleation even under relatively warm conditions (278 and 292 K) could be explained by the ternary system involving ammonia when sulfuric acid concentrations exceed several 10^7 cm^{-3} although our nucleation rates are much lower than the ones reported by *Chen et al.* [2012]. However, the study by *Chen et al.* [2012] cannot be directly compared to this one due to the possible presence of amines (or oxidized organics) during the ambient measurements and also due to the fact that they reported particle formation rates for a smaller diameter of 1 nm. When comparing our data at 292 and 298 K to the results by *Glasoe et al.* [2015] very good agreement can be found for the ternary system with ammonia.

Finally, our data demonstrate how tiny levels of ammonia (e.g., several pptv at 208 K) can influence the magnitude of nucleation rates and overwhelm the effect of IIN at even higher mixing ratios (e.g., ~100 pptv at 248 K). Therefore, there is clearly a need for the development of analytical techniques that are capable of quantifying ammonia at pptv (and ideally even at sub-pptv) levels for atmospheric measurements.

Acknowledgments

We would like to thank CERN for supporting CLOUD with important technical and financial resources and for providing a particle beam from the CERN Proton Synchrotron. We also thank P. Carrie, L.-P. De Menezes, J. Dumollard, K. Ivanova, F. Josa, I. Krasin, R. Kristic, A. Laassiri, O.S. Maksumov, B. Marichy, H. Martinati, S.V. Mizin, R. Sitals, A. Wasem, and M. Wilhelmsson for their important contributions to the experiment. We thank T. Olenius for helpful discussion. This research has received funding from the EC Seventh Framework Programme (Marie Curie Initial Training Networks "CLOUD-ITN" 215072 and "CLOUD-TRAIN" 316662, ERC-Starting "MOCAPAF" grant no. 57360 and ERC-Advanced "ATMNUCLE" grant 227463), the German Federal Ministry of Education and Research (projects 01LK0902A and 01LK1222A), the Swiss National Science Foundation (Projects 200020_135307, 206620_130527, and 206620_141278), the Väisälä Foundation, the U.S. National Science Foundation grants (AGS1447056 and AGS1439551), the U.S. Department of Energy (contract DE-SC0014469), and the Academy of Finland via the Centre of Excellence Programme (project 1118615, grants 1133872 and 251007). The data presented in this paper are available by contacting the corresponding author A. K. (kuerten@iau.uni-frankfurt.de).

References

Almeida, J., et al. (2013), Molecular understanding of sulphuric acid-amine particle nucleation in the atmosphere, *Nature*, *502*(7471), 359–363, doi:10.1038/nature12663.

Andreae, M. O., and P. J. Crutzen (1997), Atmospheric aerosols: Biogeochemical sources and role in atmospheric chemistry, *Science*, *276*(5315), 1052–1058, doi:10.1126/science.276.5315.1052.

Ball, S. M., D. R. Hanson, F. L. Eisele, and P. H. McMurry (1999), Laboratory studies of particle nucleation: Initial results for H_2SO_4, H_2O, and NH_3 vapors, *J. Geophys. Res.*, *104*, 23,709–23,718, doi:10.1029/1999JD900411.

Benson, D. R., M. E. Erupe, and S.-H. Lee (2009), Laboratory-measured H_2SO_4-H_2O-NH_3 ternary homogeneous nucleation rates: Initial observations, *Geophys. Res. Lett.*, *36*, L15818, doi:10.1029/2009GL038728.

Bianchi, F., J. Dommen, S. Mathot, and U. Baltensperger (2012), On-line determination of ammonia at low pptv mixing ratios in the CLOUD chamber, *Atmos. Meas. Tech.*, *5*(7), 1719–1725, doi:10.5194/amt-5-1719-2012.

Bianchi, F., et al. (2016), New particle formation in the free troposphere: A question of chemistry and timing, *Science*, *352*(6289), 1109–1112 doi:10.1126/science.aad5456.

Boulon, J., et al. (2010), New particle formation and ultrafine charged aerosol climatology at a high altitude site in the Alps (Jungfraujoch, 3580 m a.s.l., Switzerland), *Atmos. Chem. Phys.*, *10*(19), 9333–9349, doi:10.5194/acp-10-9333-2010.

Brock, C. A., P. Hamill, J. C. Wilson, H. H. Jonsson, and K. R. Chan (1995), Particle formation in the upper tropical troposphere: A source of nuclei for the stratospheric aerosol, *Science*, *270*(5242), 1650–1653, doi:10.1126/science.270.5242.1650.

Brock, C. A., et al. (2002), Particle growth in the plumes of coal-fired power plants, *J. Geophys. Res.*, *107*(D12), 4155, doi:10.1029/2001JD001062.

Bzdek, B. R., D. P. Ridge, and M. V. Johnston (2010), Amine exchange into ammonium bisulfate and ammonium nitrate nuclei, *Atmos. Chem. Phys.*, *10*(8), 3495–3503, doi:10.5194/acp-10-3495-2010.

Chen, M., et al. (2012), Acid–base chemical reaction model for nucleation rates in the polluted atmospheric boundary layer, *Proc. Natl. Acad. Sci. U.S.A.*, *109*(46), 18,713–18,718, doi:10.1073/pnas.1210285109.

Clarisse, L., C. Clerbaux, F. Dentener, D. Hurtmans, and P.-F. Coheur (2009), Global ammonia distribution derived from infrared satellite observations, *Nat. Geosci.*, *2*, 479–483, doi:10.1038/ngeo551.

Clarke, A. D., F. Eisele, V. N. Kapustin, K. Moore, D. Tanner, L. Mauldin, M. Litchy, B. Lienert, M. A. Carroll, and G. Albercook (1999), Nucleation in the equatorial free troposphere: Favorable environments during PEM-Tropics, *J. Geophys. Res.*, *104*, 5735–5744, doi:10.1029/98JD02303.

Coffman, D. J., and D. A. Hegg (1995), A preliminary study of the effect of ammonia on particle nucleation in the marine boundary layer, *J. Geophys. Res.*, *100*, 7147–7160, doi:10.1029/94JD03253.

de Reus, M., J. Ström, J. Curtius, L. Pirjola, E. Vignati, F. Arnold, H. C. Hansson, M. Kulmala, J. Lelieveld, and F. Raes (2000), Aerosol production and growth in the upper free troposphere, *J. Geophys. Res.*, *105*, 24,751–24,762, doi:10.1029/2000JD900382.

Dunne, E. M., et al. (2016), Global particle formation from CERN CLOUD measurements, *Science*, doi:10.1126/science.aaf2649.

Duplissy, J., et al. (2016), Effect of ions on sulfuric acid-water binary particle formation: 2. Experimental data and comparison with QC-normalized classical nucleation theory, *J. Geophys. Res. Atmos.*, *121*, 1752–1775, doi:10.1002/2015JD023539.

Ehn, M., et al. (2011), An instrumental comparison of mobility and mass measurements of atmospheric small ions, *Aerosol Sci. Technol.*, *45*(4), 522–532, doi:10.1080/02786826.2010.547890.

Ehrhart, S., and J. Curtius (2013), Influence of aerosol lifetime on the interpretation of nucleation experiments with respect to the first nucleation theorem, *Atmos. Chem. Phys.*, *13*(22), 11,465–11,471, doi:10.5194/acp-13-11465-2013.

Ehrhart, S., et al. (2016), Comparison of the SAWNUC model with CLOUD measurements of sulphuric acid-water nucleation, *J. Geophys. Res. Atmos.*, *121*, doi:10.1002/2015JD023723.

Erupe, M. E., A. A. Viggiano, and S.-H. Lee (2011), The effect of trimethylamine on atmospheric nucleation involving H_2SO_4, *Atmos. Chem. Phys.*, *11*(10), 4767–4775, doi:10.5194/acp-11-4767-2011.

Franchin, A., et al. (2015), Experimental investigation of ion-ion recombination under atmospheric conditions, *Atmos. Chem. Phys.*, *15*(13), 7203–7216, doi:10.5194/acp-15-7203-2015.

Froyd, K. D., and E. R. Lovejoy (2012), Bond energies and structures of ammonia-sulfuric acid positive cluster ions, *J. Phys. Chem. A*, *116*(24), 5886–5899, doi:10.1021/jp209908f.

Glasoe, W. A., K. Volz, B. Panta, N. Freshour, R. Bachman, D. R. Hanson, P. H. McMurry, and C. Jen (2015), Sulfuric acid nucleation: An experimental study of the effect of seven bases, *J. Geophys. Res. Atmos.*, *120*, 1933–1950, doi:10.1002/2014JD022730.

Hanson, D. R., and F. L. Eisele (2002), Measurement of prenucleation molecular clusters in the NH_3, H_2SO_4, H_2O system, *J. Geophys. Res.*, *107*(D12), 4158, doi:10.1029/2001JD001100.

Hanson, D. R., and E. R. Lovejoy (2006), Measurement of the thermodynamics of the hydrated dimer and trimer of sulfuric acid, *J. Phys. Chem. A*, *110*(31), 9525–9528, doi:10.1021/jp062844w.

Henschel, H., J. C. A. Navarro, T. Yli-Juuti, O. Kupiainen-Määttä, T. Olenius, I. K. Ortega, S. L. Clegg, T. Kurtén, I. Riipinen, and H. Vehkamäki (2014), Hydration of atmospherically relevant molecular clusters: Computational chemistry and classical thermodynamics, *J. Phys. Chem. A*, *118*, 2599–2611, doi:10.1021/jp500712y.

Iida, K., M. R. Stolzenburg, and P. H. McMurry (2009), Effect of working fluid on sub-2 nm particle detection with a laminar flow ultrafine condensation particle counter, *Aerosol Sci. Technol.*, *43*(1), 81–96, doi:10.1080/02786820802488194.

Israël, H. (1970), *Atmospheric Electricity*, vol. 1, Israel Program for Sci. Transl., Jerusalem.

Jen, C. N., P. H. McMurry, and D. R. Hanson (2014), Stabilization of sulfuric acid dimers by ammonia, methylamine, dimethylamine, and trimethylamine, *J. Geophys. Res. Atmos.*, *119*, 7502–7514, doi:10.1002/2014JD021592.

Junninen, H., et al. (2010), A high-resolution mass spectrometer to measure atmospheric ion composition, *Atmos. Meas. Tech.*, *3*(4), 1039–1053, doi:10.5194/amt-3-1039-2010.

Kazil, J., R. G. Harrison, and E. R. Lovejoy (2008), Tropospheric new particle formation and the role of ions, in *Planetary Atmospheric Electricity*, vol. 30, pp. 241–255, Springer, New York, doi:10.1007/978-0-387-87664-1_15.

Kirkby, J., et al. (2011), Role of sulphuric acid, ammonia and galactic cosmic rays in atmospheric aerosol nucleation, *Nature*, *476*(7361), 429–435, doi:10.1038/nature10343.

Kirkby, J., et al. (2016), Ion-induced nucleation of pure biogenic particles, *Nature*, *533*(7604), 521–526, doi:10.1038/nature17953.

Korhonen, P., M. Kulmala, A. Laaksonen, Y. Viisanen, R. McGraw, and J. H. Seinfeld (1999), Ternary nucleation of H_2SO_4, NH_3, and H_2O in the atmosphere, *J. Geophys. Res.*, *104*, 26,349–26,353, doi:10.1029/1999JD900784.

Krupa, S.-V. (2003), Effects of atmospheric ammonia (NH_3) on terrestrial vegetation: A review, *Environ. Pollut.*, *124*(2), 179–221, doi:10.1016/S0269-7491(02)00434-7.

Kuang, C., P. H. McMurry, A. V. McCormick, and F. L. Eisele (2008), Dependence of nucleation rates on sulfuric acid vapor concentration in diverse atmospheric locations, *J. Geophys. Res.*, *113*, D10209, doi:10.1029/2007JD009253.

Kulmala, M., H. Vehkamäki, T. Petäjä, M. Dal Maso, A. Lauri, V.-M. Kerminen, W. Birmili, and P. H. McMurry (2004), Formation and growth rates of ultrafine atmospheric particles: A review of observations, *J. Aerosol Sci.*, *35*(2), 143–176, doi:10.1016/j.jaerosci.2003.10.003.

Kulmala, M., et al. (2013), Direct observations of atmospheric aerosol nucleation, *Science*, *339*(6122), 943–946, doi:10.1126/science.1227385.

Kupc, A., et al. (2011), A fibre-optic UV system for H_2SO_4 production in aerosol chambers causing minimal thermal effects, *J. Aerosol Sci.*, *42*(8), 532–543, doi:10.1016/j.jaerosci.2011.05.001.

Kupiainen-Määttä, O., T. Olenius, H. Korhonen, J. Malila, M. Dal Maso, K. Lehtinen, and H. Vehkamäki (2014), Critical cluster size cannot in practice be determined by slope analysis in atmospherically relevant applications, *J. Aerosol Sci.*, *77*, 127–144, doi:10.1016/j.jaerosci.2014.07.005.

Kürten, A., L. Rondo, S. Ehrhart, and J. Curtius (2011), Performance of a corona ion source for measurement of sulfuric acid by chemical ionization mass spectrometry, *Atmos. Meas. Tech.*, *4*(3), 437–443, doi:10.5194/amt-4-437-2011.

Kürten, A., L. Rondo, S. Ehrhart, and J. Curtius (2012), Calibration of a chemical ionization mass spectrometer for the measurement of gaseous sulfuric acid, *J. Phys. Chem. A*, *116*(24), 6375–6386, doi:10.1021/jp212123n.

Kürten, A., et al. (2014), Neutral molecular cluster formation of sulfuric acid-dimethylamine observed in real-time under atmospheric conditions, *Proc. Natl. Acad. Sci. U.S.A.*, *111*(42), 15,019–15,024, doi:10.1073/pnas.1404853111.

Kürten, A., et al. (2015), Thermodynamics of the formation of sulfuric acid dimers in the binary (H_2SO_4-H_2O) and ternary (H_2SO_4-H_2O-NH_3) system, *Atmos. Chem. Phys.*, *15*(18), 10,701–10,721, doi:10.5194/acp-15-10701-2015.

Kurtén, T., V. Loukonen, H. Vehkamäki, and M. Kulmala (2008), Amines are likely to enhance neutral and ion-induced sulfuric acid-water nucleation in the atmosphere more effectively than ammonia, *Atmos. Chem. Phys.*, *8*(14), 4095–4103, doi:10.5194/acp-8-4095-2008.

Laakso, L., T. Hussein, P. Aarnio, M. Komppula, V. Hiltunen, Y. Viisanen, and M. Kulmala (2003), Diurnal and annual characteristics of particle mass and number concentrations in urban, rural and Arctic environments in Finland, *Atmos. Environ.*, *37*(19), 2629–2641, doi:10.1016/S1352-2310(03)00206-1.

Larsen, L., B. Roth, R. Van Dingenen, and F. Raes (1997), Photolytic aerosol formation in SO_2-HNO_2-H_2O-air mixtures, with and without NH_3, *J. Aerosol Sci.*, *28*(S1), 719–720, doi:10.1016/S0021-8502(97)85358-X.

Lee, S.-H., J. M. Reeves, J. C. Wilson, D. E. Hunton, A. A. Viggiano, T. M. Miller, J. O. Ballenthin, and L. R. Lait (2003), Particle formation by ion nucleation in the upper troposphere and lower stratosphere, *Science*, *301*(5641), 1886–1889, doi:10.1126/science.1087236.

Lohmann, U., and J. Feichter (2005), Global indirect aerosol effects: A review, *Atmos. Chem. Phys.*, *5*(3), 715–737, doi:10.5194/acp-5-715-2005.

Lovejoy, E. R., J. Curtius, and K. D. Froyd (2004), Atmospheric ion-induced nucleation of sulfuric acid and water, *J. Geophys. Res.*, *109*, D08204, doi:10.1029/2003JD004460.

Malila, J., R. McGraw, A. Laaksonen, and K. E. J. Lehtinen (2015), Communication: Kinetics of scavenging of small, nucleating clusters: First nucleation theorem and sum rules, *J. Chem. Phys.*, *142*, 011102, doi:10.1063/1.4905213.

Manninen, H. E., T. Nieminen, I. Riipinen, T. Yli-Juuti, S. Gagné, E. Asmi, P. P. Aalto, T. Petäjä, V.-M. Kerminen, and M. Kulmala (2009), Charged and total particle formation and growth rates during EUCAARI 2007 campaign in Hyytiälä, *Atmos. Chem. Phys.*, *9*(12), 4077–4089, doi:10.5194/acp-9-4077-2009.

Mauldin, R. L., III, D. J. Tanner, J. A. Heath, B. J. Huebert, and F. L. Eisele (1999), Observations of H_2SO_4 and MSA during PEM-Tropics-A, *J. Geophys. Res.*, *104*, 5801–5816, doi:10.1029/98JD02612.

McGrath, M. J., T. Olenius, I. K. Ortega, V. Loukonen, P. Paasonen, T. Kurtén, M. Kulmala, and H. Vehkamäki (2012), Atmospheric cluster dynamics code: A flexible method for solution of the birth-death equations, *Atmos. Chem. Phys.*, *12*(5), 2345–2355, doi:10.5194/acp-12-2345-2012.

Merikanto, J., D. V. Spracklen, G. W. Mann, S. J. Pickering, and K. S. Carslaw (2009), Impact of nucleation on global CCN, *Atmos. Chem. Phys.*, *9*(21), 8601–8616, doi:10.5194/acp-9-8601-2009.

Metzger, A., et al. (2010), Evidence for the role of organics in aerosol particle formation under atmospheric conditions, *Proc. Natl. Acad. Sci. U.S.A.*, *107*(15), 6646–6651, doi:10.1073/pnas.0911330107.

Mirme, S., and A. Mirme (2013), The mathematical principles and design of the NAIS – a spectrometer for the measurement of cluster ion and nanometer aerosol size distributions, *Atmos. Meas. Tech.*, *6*(4), 1061–1071, doi:10.5194/amt-6-1061-2013.

Nel, A. (2005), Air pollution–related illness: Effects of particles, *Science*, *308*(5723), 804–806, doi:10.1126/science.1108752.

Norman, M., A. Hansel, and A. Wisthaler (2007), O_2^+ as reagent ion in the PTR-MS instrument: Detection of gas-phase ammonia, *Int. J. Mass Spectrom.*, *265*(2-3), 382–387, doi:10.1016/j.ijms.2007.06.010.

O'Dowd, C. D., M. Geever, M. K. Hill, M. H. Smith, and S. G. Jennings (1998), New particle formation: Nucleation rates and spatial scales in the clean marine coastal environment, *Geophys. Res. Lett.*, *25*, 1661–1664, doi:10.1029/98GL01005.

Olenius, T., et al. (2013), Comparing simulated and experimental molecular cluster distributions, *Faraday Discuss.*, *165*, 75–89, doi:10.1039/C3FD00031A.

Ortega, I. K., O. Kupiainen, T. Kurtén, T. Olenius, O. Wilkman, M. J. McGrath, V. Loukonen, and H. Vehkamäki (2012), From quantum chemical formation free energies to evaporation rates, *Atmos. Chem. Phys.*, *12*(1), 225–235, doi:10.5194/acp-12-225-2012.

Ortega, I. K., T. Olenius, O. Kupiainen-Määttä, V. Loukonen, T. Kurtén, and H. Vehkamäki (2014), Electrical charging changes the composition of sulfuric acid-ammonia/dimethylamine clusters, *Atmos. Chem. Phys.*, *14*(15), 7995–8007, doi:10.5194/acp-14-7995-2014.

Panta, B., W. A. Glasoe, J. H. Zollner, K. K. Carlson, and D. R. Hanson (2012), Computational fluid dynamics of a cylindrical nucleation flow reactor with detailed cluster thermodynamics, *J. Phys. Chem. A*, *116*, 10,122–10,134, doi:10.1021/jp302444y.

Praplan, A. P., F. Bianchi, J. Dommen, and U. Baltensperger (2012), Dimethylamine and ammonia measurements with ion chromatography during the CLOUD4 campaign, *Atmos. Meas. Tech.*, *5*(9), 2161–2167, doi:10.5194/amt-5-2161-2012.

Raes, F., and A. Janssens (1985), Ion-induced aerosol formation in a H_2O-H_2SO_4 system – extension of the classical theory and search for experimental evidence, *J. Aerosol Sci.*, *16*(3), 217–227, doi:10.1016/0021-8502(85)90028-X.

Riccobono, F., et al. (2012), Contribution of sulfuric acid and oxidized organic compounds to particle formation and growth, *Atmos. Chem. Phys.*, *12*(20), 9427–9439, doi:10.5194/acp-12-9427-2012.

Riccobono, F., et al. (2014), Oxidation products of biogenic emissions contribute to nucleation of atmospheric particles, *Science*, *344*(6185), 717–721, doi:10.1126/science.1243527.

Rose, C., et al. (2015a), Major contribution of neutral clusters to new particle formation at the interface between the boundary layer and the free troposphere, *Atmos. Chem. Phys.*, *15*(6), 3413–3428, doi:10.5194/acp-15-3413-2015.

Rose, C., et al. (2015b), Frequent nucleation events at the high altitude station of Chacaltaya (5240 m a.s.l.), Bolivia, *Atmos. Environ.*, *102*, 18–29, doi:10.1016/j.atmosenv.2014.11.015.

Schnitzhofer, R., et al. (2014), Characterisation of organic contaminants in the CLOUD chamber at CERN, *Atmos. Meas. Tech.*, *7*(7), 2159–2168, doi:10.5194/amt-7-2159-2014.

Schobesberger, S., et al. (2013), Molecular understanding of atmospheric particle formation from sulfuric acid and large oxidized organic molecules, *Proc. Natl. Acad. Sci. U.S.A.*, *110*(43), 17,223–17,228, doi:10.1073/pnas.1306973110.

Schobesberger, S., et al. (2015), On the composition of ammonia-sulfuric-acid ion clusters during aerosol particle formation, *Atmos. Chem. Phys.*, *15*(1), 55–78, doi:10.5194/acp-15-55-2015.

Sihto, S.-L., et al. (2006), Atmospheric sulphuric acid and aerosol formation: Implications from atmospheric measurements for nucleation and early growth mechanisms, *Atmos. Chem. Phys.*, *6*(12), 4079–4091, doi:10.5194/acp-6-4079-2006.

Stanier, C. O., A. Y. Khlystov, and S. N. Pandis (2004), Nucleation events during the Pittsburgh air quality study: Description and relation to key meteorological, gas phase, and aerosol parameters, *Aerosol Sci. Technol.*, *38*(S1), 253–264, doi:10.1080/02786820390229570.

Su, T., and W. J. Chesnavich (1982), Parametrization of the ion-polar molecule collision rate constant by trajectory calculations, *J. Chem. Phys.*, *76*(10), 5183–5185, doi:10.1063/1.442828.

Torpo, L., T. Kurtén, H. Vehkamäki, K. Laasonen, M. R. Sundberg, and M. Kulmala (2007), Significance of ammonia in growth of atmospheric nanoclusters, *J. Phys. Chem. A*, *111*(42), 10,671–10,674, doi:10.1021/jp0741307.

Vaittinen, O., M. Metsälä, S. Persijn, M. Vainio, and L. Halonen (2014), Adsorption of ammonia on treated stainless steel and polymer surfaces, *Appl. Phys. B*, *115*(2), 185–196, doi:10.1007/s00340-013-5590-3.

Vanhanen, J., J. Mikkilä, K. Lehtipalo, M. Sipilä, H. E. Manninen, E. Siivola, T. Petäjä, and M. Kulmala (2011), Particle size magnifier for nano-CN detection, *Aerosol Sci. Technol.*, *45*(4), 533–542, doi:10.1080/02786826.2010.547889.

Voigtländer, J., J. Duplissy, L. Rondo, A. Kürten, and F. Stratmann (2012), Numerical simulations of mixing conditions and aerosol dynamics in the CERN CLOUD chamber, *Atmos. Chem. Phys.*, *12*(4), 2205–2214, doi:10.5194/acp-12-2205-2012.

Weber, R. J., J. J. Marti, P. H. McMurry, F. L. Eisele, D. J. Tanner, and A. Jefferson (1996), Measured atmospheric new particle formation rates: Implications for nucleation mechanisms, *Chem. Eng. Commun.*, *151*, 53–64, doi:10.1080/00986449608936541.

Weber, R. J., P. H. McMurry, L. Mauldin, D. J. Tanner, F. L. Eisele, F. J. Brechtel, S. M. Kreidenweis, G. L. Kok, R. D. Schillawski, and D. Baumgardner (1998), A study of new particle formation and growth involving biogenic and trace gas species measured during ACE 1, *J. Geophys. Res.*, *103*, 16,385–16,396, doi:10.1029/97JD02465.

Weber, R. J., P. H. McMurry, R. L. Mauldin III, D. J. Tanner, and F. L. Eisele (1999), New particle formation in the remote troposphere: A comparison of observations at various sites, *Geophys. Res. Lett.*, *26*, 307–310, doi:10.1029/1998GL900308.

Weigel, R., et al. (2011), In situ observations of new particle formation in the tropical upper troposphere: The role of clouds and the nucleation mechanism, *Atmos. Chem. Phys.*, *11*(18), 9983–10,010, doi:10.5194/acp-11-9983-2011.

Wimmer, D., et al. (2013), Performance of diethylene glycol based particle counters in the sub-3 nm size range, *Atmos. Meas. Tech.*, *6*(7), 1793–1804, doi:10.5194/amt-6-1793-2013.

Wimmer, D., et al. (2015), Technical note: Using DEG-CPCs at upper tropospheric temperatures, *Atmos. Chem. Phys.*, *15*(13), 7547–7555, doi:10.5194/acp-15-7547-2015.

Yu, F., and R. P. Turco (2000), Ultrafine aerosol formation via ion-mediated nucleation, *Geophys. Res. Lett.*, *27*, 883–886, doi:10.1029/1999GL011151.

Yu, H., R. McGraw, and S.-H. Lee (2012), Effects of amines on formation of sub-3 nm particles and their subsequent growth, *Geophys. Res. Lett.*, *39*, L02807, doi:10.1029/2011GL050099.

Zhang, R., I. Suh, J. Zhao, D. Zhang, E. C. Fortner, X. Tie, L. T. Molina, and M. J. Molina (2004), Atmospheric new particle formation enhanced by organic acids, *Science*, *304*(5676), 1487–1490, doi:10.1126/science.1095139.

Zollner, J. H., W. A. Glasoe, B. Panta, K. K. Carlson, P. H. McMurry, and D. R. Hanson (2012), Sulfuric acid nucleation: Power dependencies, variation with relative humidity, and effect of bases, *Atmos. Chem. Phys.*, *12*(10), 4399–4411, doi:10.5194/acp-12-4399-2012.